

**EXPERIMENTING ON THE EFFECTIVENESS OF RIP RAP ROCKS AS AN
ENERGY DISSIPATING STRUCTURE**

By

AHMAD WARIZ BIN ABD WAHID

Final draft submitted in partial
Fulfillment of the requirements for the
Bachelor of Engineering (Hons)
Civil Engineering

May 31, 2005

Universiti Teknologi PETRONAS
Bandar Seri Iskandar
31750 Tronoh
Perak Darul Ridzuan

CERTIFICATION OF APPROVAL

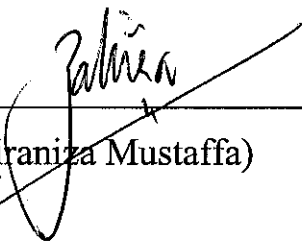
Experimenting the Effectiveness of Rip Rap Rocks as an Energy Dissipator

by

Ahmad Wariz bin Abd Wahid

A project dissertation submitted to the
Civil Engineering Program
Universiti Teknologi PETRONAS
in partial fulfillment of the requirements for the
BACHELOR OF ENGINEERING (Hons)
(CIVIL ENGINEERING)

Approved by,



(Zahiraniza Mustaffa)

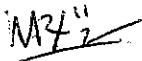
UNIVERSITI TEKNOLOGI PETRONAS

TRONOH, PERAK

JUNE 2005

CERTIFICATION OF ORIGINALITY

This is to certify that I am responsible for the work submitted in this project, that the original work is my own except as specified in the references and acknowledgements, and the original work contained herein have not been taken or done by unspecified sources or persons.



AHMAD WARIZ BIN ABD WAHID

ABSTRACT

The design of the energy dissipator probably includes more options than any other phase of a spillway design. The selection of the type and design details of the dissipater is largely dependant upon the pertinent characteristics of the site, the magnitude of energy to be dissipated and to a lesser use. Good judgment is imperative to assure that all requirements of the particular project are met. Regardless of the type of dissipater selected, any spillway energy dissipator must operate safely at high discharges for extended periods of time. This study presents a detailed explanation on the various designs of rip rap rock energy dissipators and their applications on a spillway. The importance of energy dissipator on a spillway is to protect structures downstream from a spillway. The purpose of energy dissipator is to dissipate energy from the flow of water so that is not strong enough to harm or damage downstream structures of a dam. Thus, the objectives of this study are as follows, to design several designs of rip rap rocks energy dissipating structures, to perform experiments on the model using various flows and to compare the performance of the designed rip rap models. Three designs have been selected for modeling and presented in this report. The three models were constructed with reference to the rip rap design located on the spillway on the Kenyir Dam in Terengganu, baffled blocks basin designs, baffled apron drop design and gabion designs. These models will then be experimented in a flume available in the laboratory using various flows to determine the most effective energy dissipator. Upon experimentation, it is understood that the model that was built with reference to the design of the energy dissipator located at the Kenyir Dam, was found to be the most effective energy dissipator for it was able to dissipate the most amount of energy compared to the other models that were constructed. Furthermore, it had a larger surface roughness area compared to the other models as well.

ACKNOWLEDGEMENT

Upon completing this final year project, first and foremost, I would like thank the mighty Allah for giving me strength, guidance and good health throughout the commission of this project.

My deepest appreciation goes to my supervisor, Miss Zahiraniza bt Mustaffa, for her guidance, encouragement and patience that helped to inspire me to complete this project. Without her dedication and assistance, this project would not have reached this page.

A token of appreciation also goes to the laboratory assistants, Mr Johan and Mr Zaini for their assistance during the experiments in the laboratory.

To my beloved parents, Abd Wahid Abu and Zarina Ahamad Osman, thank you for always being there for me in my hour of need.

Finally, special thanks goes to all my friends for their great ideas and support which helped me complete this project.

Your kindness and support is highly appreciated and would never be forgotten.

TABLE OF CONTENTS

ABSTRACT	1
ACKNOWLEDGEMENT	2
TABLE OF CONTENTS	3
LIST OF FIGURES	6
LIST OF TABLES	9
CHAPTER 1	10
INTRODUCTION	10
1.1 Background	10
1.2 Problem Statement	10
1.3 Objective	11
CHAPTER 2	12
LITERATURE REVIEW	12
2.1 Rip Rap Rock	12
2.2 Gabions	13
2.2.1 Wire and Mesh	13
2.2.2 Filling Material	14
2.3 Stilling Basins	14
2.3.1 Basin I	15
2.3.2 Basin II	15

2.3.3 Basin III	17
2.3.4 Basin IV	17
2.3.5 Basin V	18
2.4 Spillways	20
2.4.1 Purpose of Spillways	20
2.4.2 Types of Spillways	20
2.5 Application of Energy Equation	21
2.6 Flow over Scattered Roughness Elements	23
2.6.1 Types of Flow over Rough Boundaries	24
CHAPTER 3	26
METHODOLOGY	26
3.1 Tools/Equipments	26
3.2 Spillway Model Without Rip Rap	26
3.3 Spillway Model With Rip Rap Designs	27
3.3.1 Design Model 1	28
3.3.2 Design Model 2	29
3.3.3 Design Model 3	31
3.4 Materials	34
3.5 Experimental Setup	37
3.5.1 Hydraulics Flume	37
3.5.2 Hook and Point Gauge for Modular Flow Channel	38
3.5.3 Current Meter	39

3.6 Experimental Procedure	40
CHAPTER 4	42
RESULTS AND DISCUSSION	42
4.1 Water Depth Computation	43
4.1.1 Upstream Section	43
4.1.2 Downstream Section	43
4.2 Theoretical Flowrate, Q_t and Actual Flowrate, Q_a	44
4.3 Energy Loss, h_L	47
4.4 Observations	53
4.4.1 Design Model 2	53
4.4.2 Design Model 3	58
CONCLUSION	63
REFERENCE	64
APPENDIX	65

LIST OF FIGURES

Figure 1: Length of jump (Adapted from Chanson,1994)

Figure 2 : Type II basin dimensions (Adapted from Chanson,1994)

Figure 3: Minimum tailwater depths (Adapted from Chanson, 1994)

Figure 4 : Type III basin dimensions (Adapted from Chanson,1994)

Figure 5 : Type IV basin dimensions (Adapted from Chanson,1994)

Figure 6 : Type V design dimensions (Adapted from Chanson,1994)

Figure 7 : Length of jump (Adapted from Chanson,1994)

Figure 8 : Flow transition (Adapted from Chadwick and Morfett, 2002)

Figure 9: Figure depicting flow through energy dissipator

Figure 10 : Classification of flow over scattered roughness (Adapted from Ranga Raju,
2003)

Figure 11 : Model of Spillway without Rip Rap

Figure 12: Design 1: 3D view

Figure 13: Design 1: side view

Figure 14: Design 1: top view

Figure 15: Design Model 1

Figure 16: Design 2: 3D view

Figure 17: Design 2: side view

Figure 18 : Design 2 : top view

Figure 19: Design Model 3

Figure 20: Design 3: 3D view

Figure 21: Design 3: side view

Figure 22: Design 3 : top view

Figure 23: Design Model 3

Figure 24: Red limestone

Figure 25 : Granite

Figure 26 : Existing Flume used in the Experiment

Figure 27 : Experimental Setup of Flume

Figure 28: Point Gauge

Figure 29: Current Meter

Figure 30: Points of Water Depth Measurements in the Flume

Figure 31: Comparison between the Theoretical and Actual Flowrate

Figure 32: Graph of Energy Loss versus Theoretical Discharge for all models

Figure 33: Flow Variations on Design Model 1

Figure 34: Flow Variations on Design Model 2

Figure 35: Flow Variations on Design Model 3

Figure 36: Side view of Design Model 2 at $5 \text{ m}^3/\text{hr}$

Figure 37: Plan view of Design Model 2 at $5 \text{ m}^3/\text{hr}$

Figure 38: Side view if Design Model 2 at $80 \text{ m}^3/\text{hr}$

Figure 39: Plan view of Deign Model 2 at $80 \text{ m}^3/\text{hr}$

Figure 40: Side view of Downstream at $5 \text{ m}^3/\text{hr}$

Figure 41: Plan view of Downstream at 5 m³/hr

Figure 42: Side view of Downstream at 80 m³/hr

Figure 43: Plan view of Downstream at 80 m³/hr

Figure 44: Side view of Design Model 3 at 5 m³/hr

Figure 45: Plan view of Design Model 2 at 5 m³/hr

Figure 46: Side view if Design Model 2 at 80 m³/hr

Figure 47: Plan view of Deign Model 2 at 80 m³/hr

Figure 48: Side view of Downstream at 5 m³/hr

Figure 49: Plan view of Downstream at 5 m³/hr

Figure 50: Side View of Downstream at 80 m³/hr

Figure 51: Plan View of Downstream at 80 m³/hr

LIST OF TABLES

Table 1: Rip rap Minimum D50 Sizing Chart.

Table 2: Results of Experiment with Spillway without Rip Rap

Table 3: Results of Experiment with Design Model 1

Table 4: Results of Experiment with Design Model 2

Table 5: Results of Experiment with Design Model 3

CHAPTER 1

INTRODUCTION

1.1 Introduction

Construction of civil engineering works with stone or rock dates from biblical times. Stone is generally abundantly available and easily accessible. It is often available in a range of sizes from surface deposits, river banks and gravel pits, or it can be quarried from rock outcrops. Stone is strong, heavy, chemically inert and durable. These features make stone a desirable and often economic building material.

In hydraulic engineering, stone has been used for rock fill dams, breakwaters, jetties, spurs, pier protection, bank and shore protection and scour control at hydraulic structures. In the decade of the 1970's, however, with a booming world economy and significant emphasis on mega projects, there was a tendency to construct increasing number of more sophisticated reinforced concrete structures. This is not always appropriate technology. In developing countries in particular, use of locally available materials and labor intensive methods makes good socio-economic sense.

1.2 Problem Statement

The need for reinforce concrete becomes obvious when one is dealing with high velocities and large discharges. But this is not always the case. At Kenyir Dam, Terengganu, they had used rip rap rocks as an energy dissipating structure compared to the typically used stilling basins. Although theoretically, rocks are not recommended for usage when dealing with high velocities and large discharges, but the Kenyir Dam is living proof that it can be done, if it is done in a correct manner. So in this project, much investigation will be done on the design of the rip rap rocks structure as an energy dissipating structure in the dam using various rock formations and types. Furthermore, experiments will be performed on the model of the dam using various flows and

discharges to analyze the effectiveness of the rip rap rocks as an energy dissipater, compared to the stilling basins.

1.3 Objectives

The objectives of this project are summarized as follows:

1. To design several designs of rip rap rocks energy dissipating structures.
2. To perform experiments on the model using various flows.
3. To compare the performance of the designed rip rap models.

CHAPTER 2

LITERATURE REVIEW

Most of the literature review for this initial phase is geared towards identifying the current use of rip rap rocks and its functions as well as understanding the types and function of the stilling basins. Following is a brief summary of the literature reviewed.

2.1 Rip Rap Rock

Currently, rip rap rock is used for various purposes in hydraulic engineering. It has been used for rockfill dams, breakwaters, pier protection, bank and shore protection. Nevertheless, if very large discharges or velocities are to be handled, this will usually dictate the need for reinforcement concrete, because stone sizes required for stability becomes prohibitively large under these conditions. However, there are many instances of the need for smaller size structures for drainage, irrigation and water resource projects. When stone of a suitable quality and quantity is available near the site of a structure, it should be considered as a possible construction material. Advantages include simple design and construction, the absence of the need for skilled labor or quality control, and speed of construction. Of course, selection of a building material should always be based on least cost, including consideration of life of structure and operation and maintenance, but stone should never be dismissed out of hand.

But in this project, based on those designs for all those purposes, the author shall design a rip rap rock that will serve as an energy dissipator. Although, theoretically it is already stated that stone or rocks would not be an ideal choice when dealing with large flows and discharges, but observation at Kenyir Dam, Terengganu has shown that it can be done. Meaning, rip rap rock has been used as an energy dissipator. But what remain unknown is the design in which they built it and how effective does the rip rap rock work against large flows and discharges. So, in this project, a detailed analysis will be performed on the current existing designs of rip rap rocks and study the rock formations used in each

purpose. Then, the author shall construct a model based on three most effective designs and then run experiments and tests on them to identify which formation or design to be the most effective. These readings will then be compared to the stilling basins structure to identify which is the more effective energy dissipator.

2.2 Gabions

Gabions are extensively used for earth retaining structures and for hydraulic structures, for example weirs and channel linings. Chanson (1994) stated that their advantages are their stability, low cost, flexibility and porosity.

The porosity of gabions is an important factor preventing the building up of large uplift pressures. Originally, a gabion is a basket filled with earth or stone for use in fortification and engineering. The gabion technique has been known for thousands of years. Original gabions used by Egyptians were made of rushes and papyrus. In China, hydraulic engineers used extensively gabions of bamboo basketwork for over one thousand years. Gabions used as construction material consist of rockfill material enlaced by a basket or a mesh. Various filling material and container can be used.

Box gabions are rectangular cages with rockfill material. Typical gabion dimensions are heights of 0.5 to 1 m, a width equal to the height and length over height ration between 1.5 to 4 m. Long gabions are usually subdivided into cells by inserting diaphragms made of mesh panels to strengthen the gabion.

2.2.1 Wire and Mesh

The wire is normally soft steel with a zinc coating. In practice, the durability of gabion structures depends strongly upon the quality of the mesh and wires. The strength of the gabion container might be reduced by corrosion, gabion flexing and debris impacts. High quality and strengthen mesh wires can be used, for example galvanized wire, zinc coating

wire and plastic (PVC) coated wire. Note that Chinese experience showed that bamboo baskets are durable and can last five to ten years at least.

2.2.2 Filling Material

The gabion filling consists of loose or compacted rocks. In any case, the stone size of the rockfill must be equal to at least 1 to 1.5 times the mesh size but not be larger than 2/3 of the minimum dimension of the gabion. The use of small sized stone permits more economical filling of the cage and it allows a better adaptability of the gabions to deformation.

2.3 Stilling Basins

Stilling basins are structures designed to contain the hydraulic jump. They are used as an energy dissipation device. They also help to decrease the flow velocity at the exit of the basin with respect to the entry velocity. In this way, the scour below the stilling basin is kept under control.

It is very difficult to classify the possible stilling basin designs, as there is so much variation in the purpose, size and constraints of each type. There are literally hundreds of designs, most of which have been developed by careful testing in model form. It may be said that unless the energy dissipation structure under study is of relatively small size and importance, this structure is almost always tested in model form.

The following, taken from Mays (2001), are examples of several general types of stilling basins which are Basin I, II, III, IV and V.

2.3.1 Basin I

For Froude number less than 1.7, no special stilling basin is required. Channel lengths must extend beyond the point where the depth starts to change to not less than $4y_2$. These basins do not require baffle or dissipation devices. These basins are referred to as Type –I basins. For Froude numbers between 1.7 and 2.5, the type-I basin also applies. Characteristics of the type-I basins are shown in Figure 1.

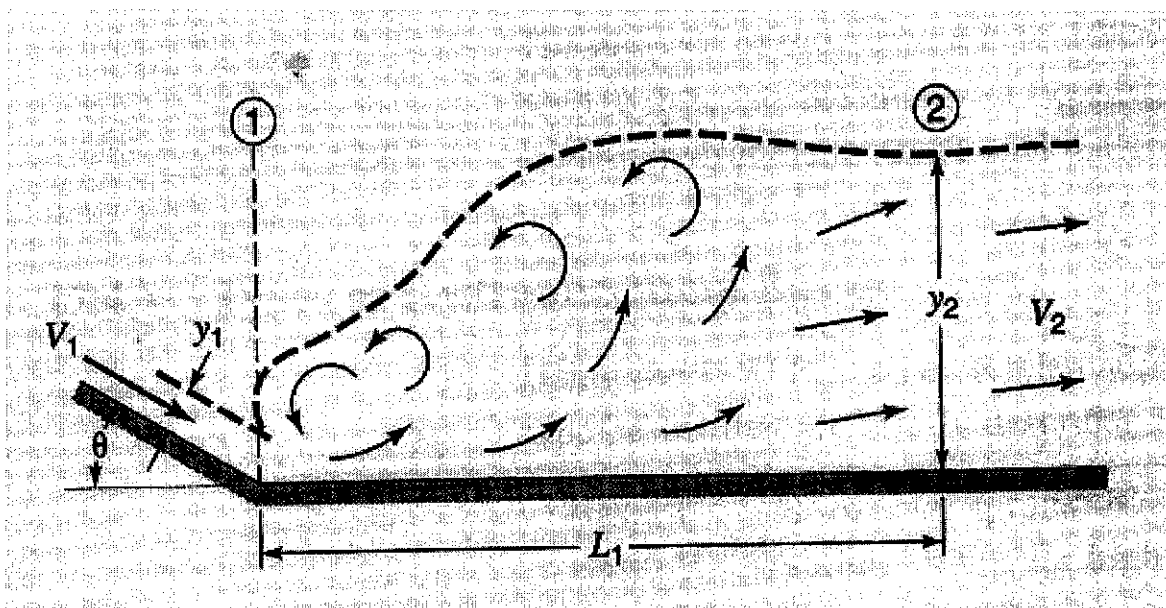


Figure 1: Length of jump (Adapted from Chanson, 1994)

2.3.2 Basin II

Basins that have been used with high earth dam and earth dam spillways are type-II basins (refer to Figure 2). These basins contain chute blocks at the upstream end and a dentated sill near the downstream end. Baffled piers are not needed because of the relatively high velocity entering the jump. These basins are for Froude numbers above 4.5 or velocities above 50 ft/s. Relationships illustrating stilling basins proportional to

minimum tailwater depths and lengths of jump, as function of Froude number, are presented in Figure 3.

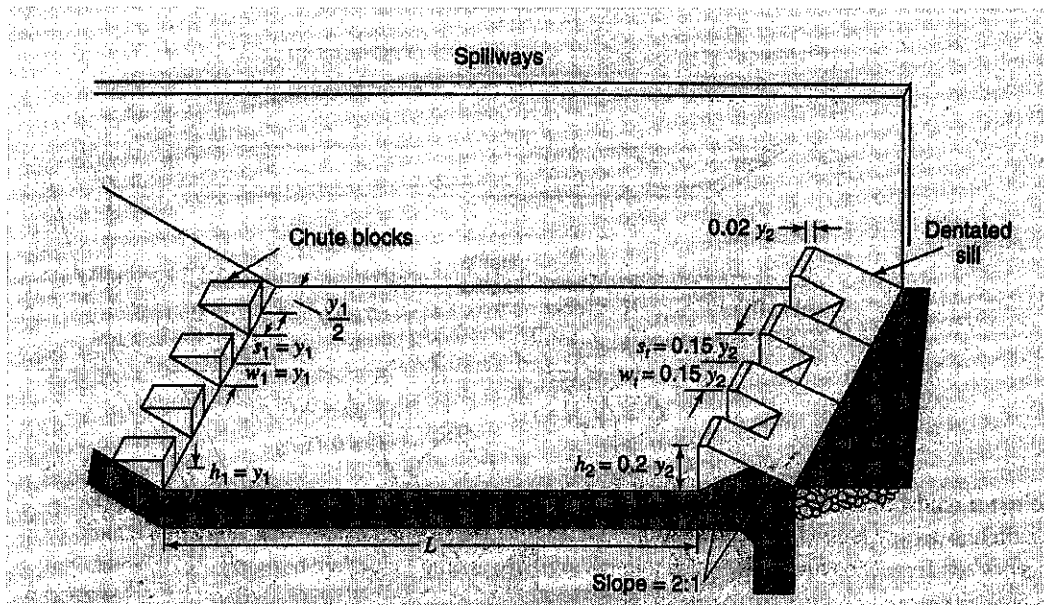


Figure 2 : Type II basin dimensions (Adapted from Chanson, 1994)

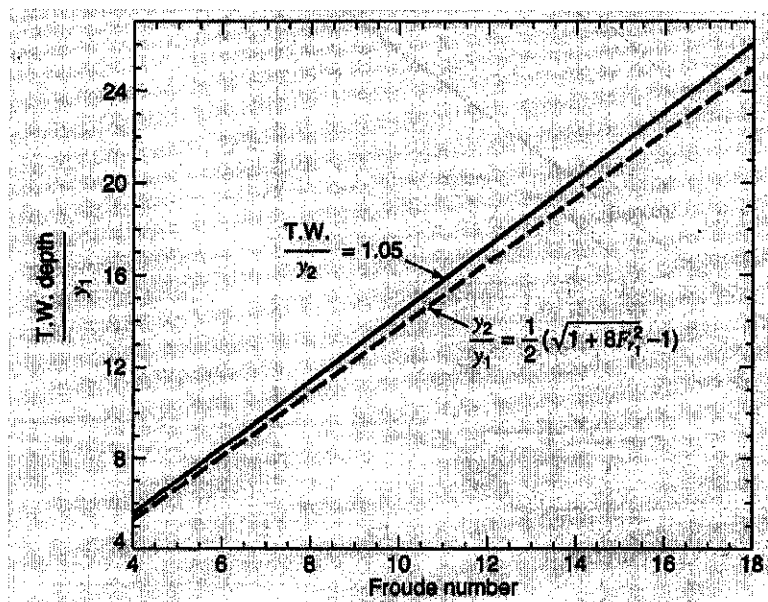


Figure 3 : Minimum tailwater depths (Adapted from Chanson, 1994)

2.3.3 Basin III

Type-III basins are shorter basins than the type-II with a simpler end sill and with baffle piers downstream of the chute blocks (See Figure 4). The incoming velocity for the type-III basin must be limited to prevent the possibility of low pressures on the baffle piers that can result in cavitation. The type-III basin length is about 60 percent of the type-II basin. Type-III basins are used on small spillways, outlet works, and small canal structures where V_1 does not exceed 50 or 60 ft/sec. and the Froude number F_1 is more than 4.5.

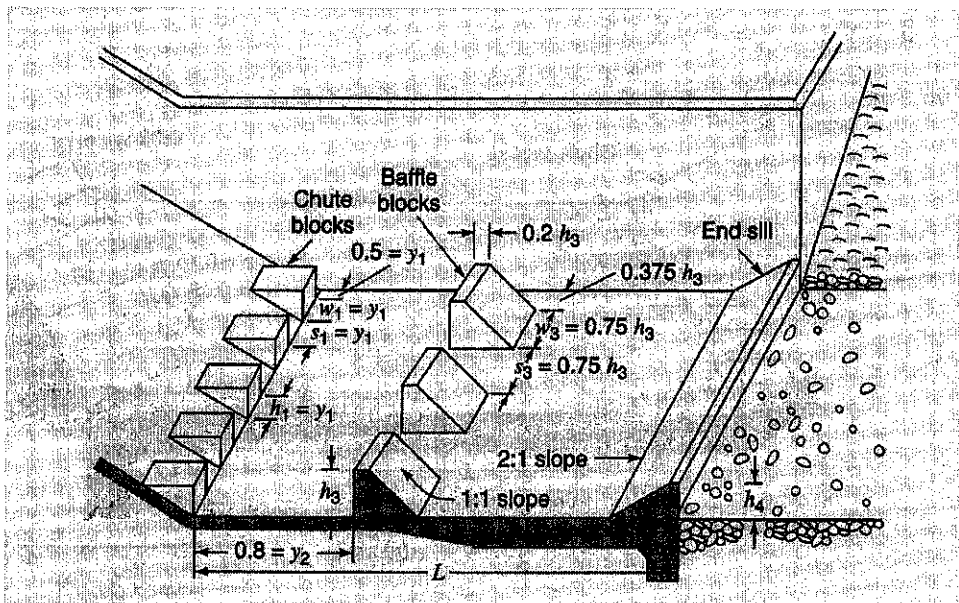


Figure 4 : Type III basin dimensions (Adapted from Chanson, 1994)

2.3.4 Basin IV

Type-IV basins are used where the Froude number is in the range of 2.5 to 4.5, which is typical of canal structures and occasionally of low dams, small outlet works, and diversion dams. In this case the hydraulic jump is not fully developed and the main concern is the waves created in the unstable hydraulic jump. These basins reduce excessive waves created in imperfect jumps. Figure 5 illustrates the characteristics of this basin along with an alternate design and wave suppressors that may be used in place of

the type-III basin. Figure 7 shows an alternative low Froude number stilling basin. The type-IV basin has large deflector blocks that are similar to but larger than chute blocks, and an optional solid end sill. The design shown in Figure 15 does not have chute blocks, but does have large baffle piers and a dentated end sill.

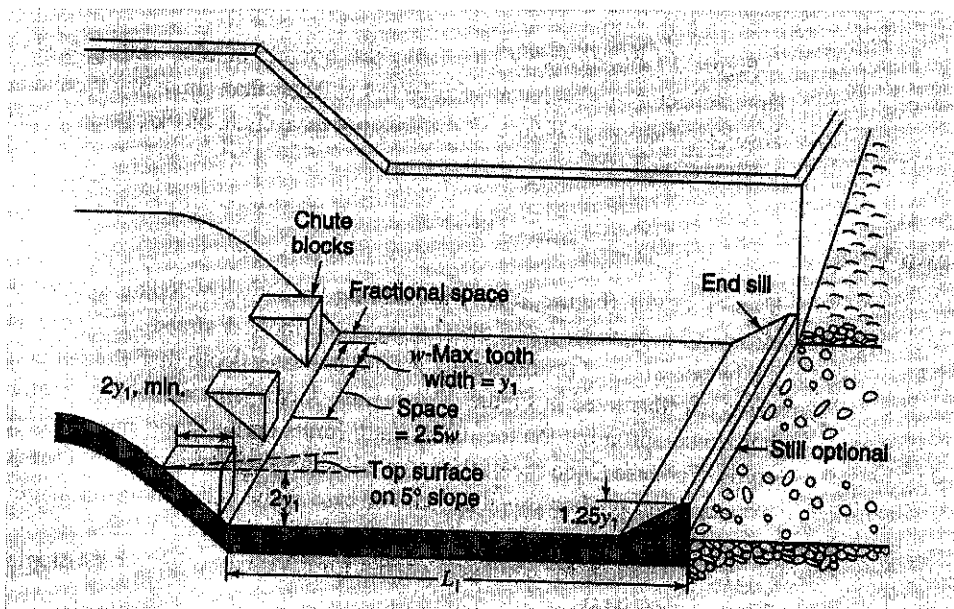


Figure 5 : Type IV basin dimensions (Adapted from Chanson, 1994)

2.3.5 Basin V

Type-V basins are stilling basins with sloping aprons, which are for use where structural economics make the sloping apron more desirable. They are usually used on high dam spillways, sloping aprons need a greater tailwater depth than the horizontal (Type-I) basins.

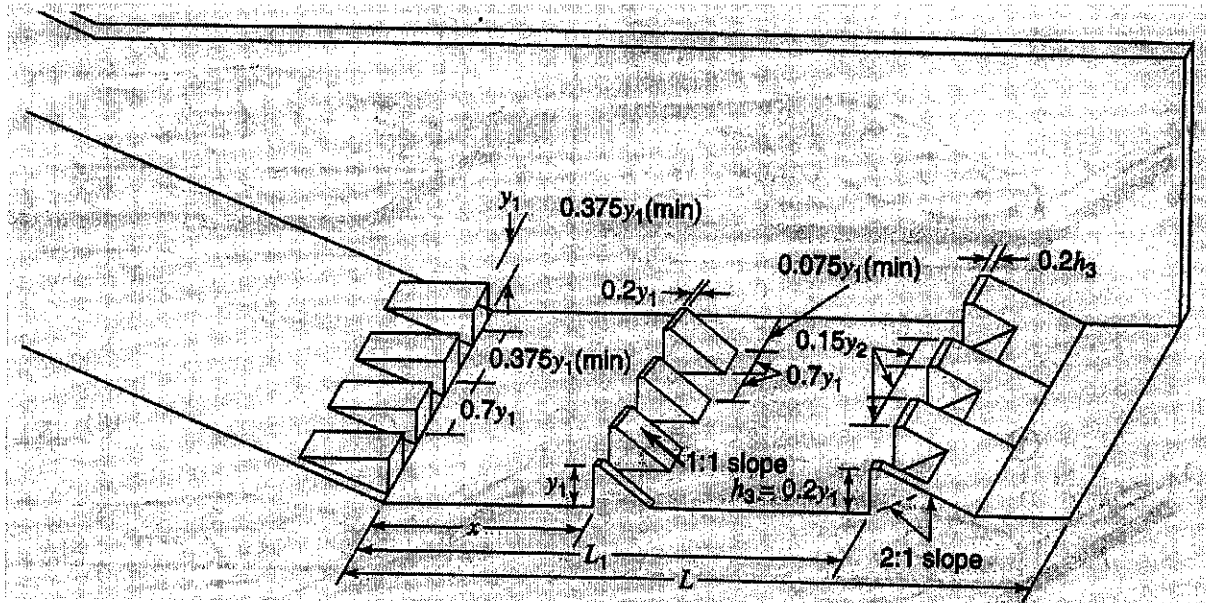


Figure 6 : Type V design dimensions (Adapted from Chanson, 1994)

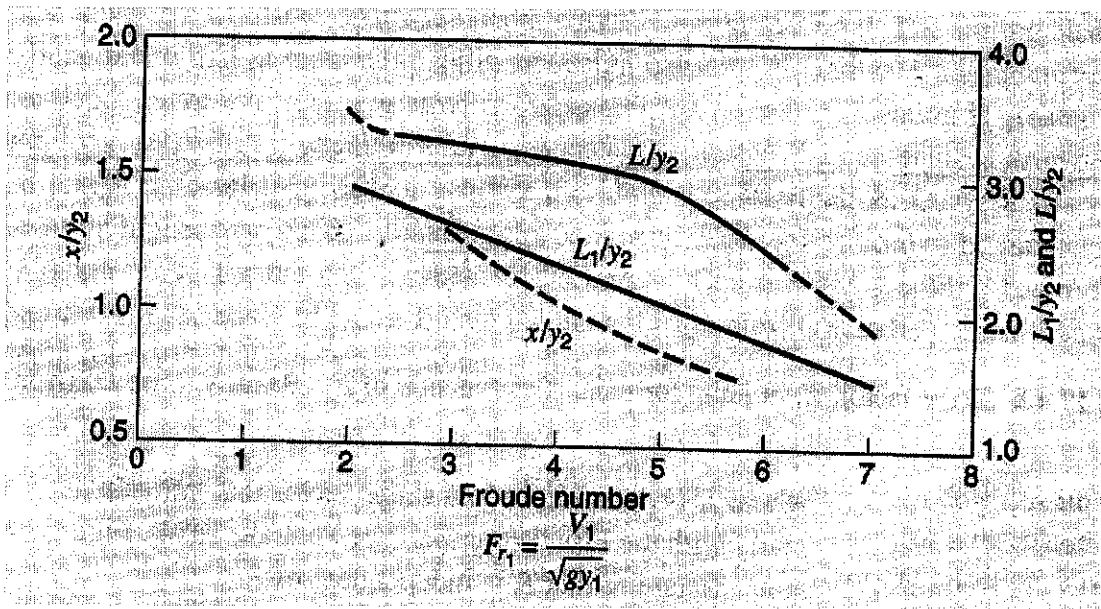


Figure 7 : Length of jump (Adapted from Chanson, 1994)

2.4 Spillways

2.4.1 *Purpose of Spillways*

Spillways are built to discharge excess river flow, during times of flood. It is done in such a manner as to insure the safety of the dam works at all time. All storage dams must be protected by a spillway. Although storage dams are relatively high dams and have a significant storage volume, it is never economically feasible to build the dam high enough to store the low frequency high discharge floods in the reservoir. Some condition must be made to get the excess flow safely through, over, or around the dam. A spillway is used for this purpose.

2.4.2 *Types of Spillway*

The type of spillway used in a certain case depends upon the type of dam, the magnitude of the spillway design discharge, the topography, and the nature of the foundation. Flow may be allowed to pass directly over a portion of a concrete gravity dam. Such a spillway is called an overflow spillway. In some cases an overflow spillway may be used with a concrete buttress dam or an arch dam. Often, however, a separate structure is used with an arched dam. In case of space limitations, a narrow arch, a side channel spillway or shaft spillway may be used. A separate structure must always be used for a rock fill or earth fill dam. In this case, a concrete chute spillway is most common. On smaller dams, a simple drop inlet or box inlet spillway may be more economical than other types.

Regardless of the type, every spillway has three basic components – a crest section, a conveyance section, and a discharge section. The crest section is the inlet to the spillway, situated at or near the reservoir level. From the crest the flow must be conveyed in a chute or a tunnel to a level near the natural river level on the downstream side of the dam. The spillway terminates in a discharge section, from which the flow re enters the channel. If necessary, the discharge section may also be the means of dissipating the excess kinetic energy of the flow.

2.5 Application of the Energy Equation

In hydraulic engineering, numerous devices like stilling basins, baffled aprons and vortex shafts are known under the collective term of energy dissipators. Their purpose is to dissipate hydraulics energy meaning to convert it mainly to heat. Dissipators are used in places where the excess hydraulic energy could cause damages such as erosion of tailwater channels, abrasion of hydraulic structures, and generation of tailwater waves or scouring. Visher and Hager (1995) reported that the term energy dissipator used by hydraulic engineers refers to devices that get rid of hydraulic energy. The important phenomenon is the annihilation of hydro-mechanical energy rather than energy conversion.

According to Chadwick and Morfett (2002), by referring to Figure 18, steady uniform flow is interrupted by the presence of a hump in the streambed. The upstream depth and the discharge at point 1 are known and it simply remains to find the depth of flow at point 2.

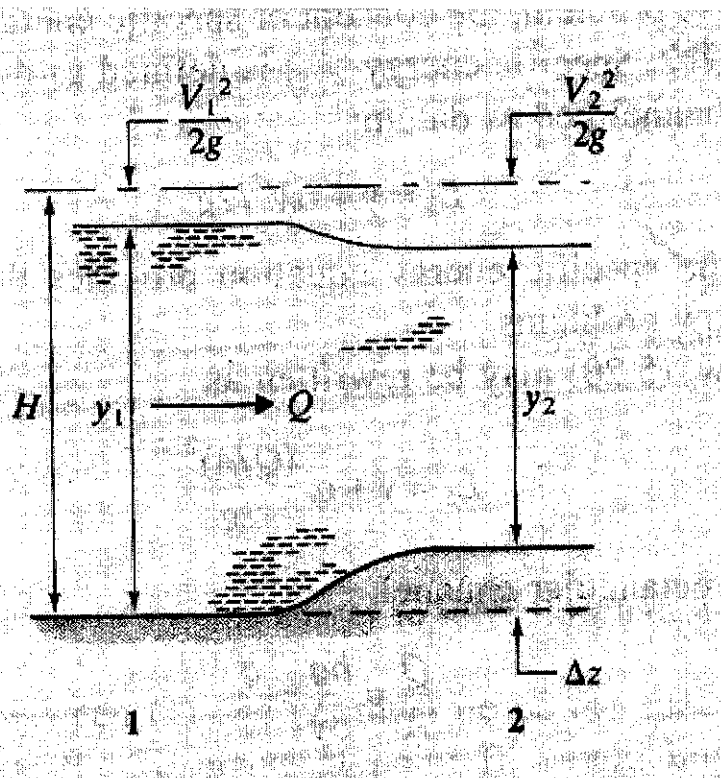


Figure 8 : Flow transition (Adapted from Chadwick and Morfett, 2002)

Applying the energy equation and assuming that frictional energy loss between 1 and 2 are negligible, then,

$$y_1 + \frac{v_1^2}{2g} = y_2 + \frac{v_2^2}{2g} + \Delta z \quad (1)$$

Where, y_1 is depth at point 1, y_2 is depth at point 2, V_1 is velocity at point 1, V_2 is velocity at point 2, Δz is difference in elevation between point 1 and 2.

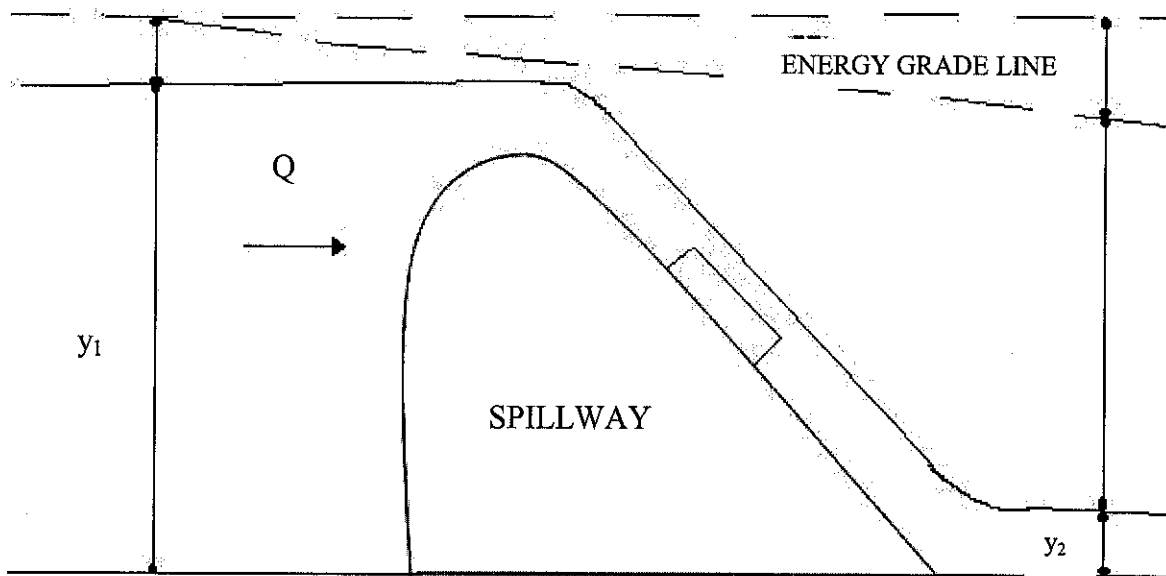


Figure 9: Figure depicting flow through energy dissipator

For this project, the same concept is applied but the conditions applied are different. For this project, the energy loss is not negligible but rather, there is no difference in elevation, hence no Δz . But rather, there is head loss, h_L , thus the energy equation becomes,

$$y_1 + \frac{v_1^2}{2g} = y_2 + \frac{v_2^2}{2g} + h_L \quad (2)$$

$$\text{If } E \text{ is given by, } E = y + \frac{v^2}{2g} \quad (3)$$

$$\text{Then, } h_L = E_1 - E_2 \quad (4)$$

This energy equation is the main equation used in this project. As the flow flows through the energy dissipator, there will be a head loss, h_L incurred and the best design is chosen based on the amount of h_L it can produce.

2.6 Flow over Scattered Roughness Elements

Various studies have been carried out in recent years on the resistance characteristics of open channels whose boundaries are studded with roughness elements of geometrical shape arranged in regular array. Cubes, hemispheres, spheres, rectangular strips, etc. have been used as the roughness elements in the above studies. The objective was to get a better understanding of the complex problem of flow over rough surfaces. The work of Morris (1995), as referred from Ranga Raju (2003), deserves special mention in this regard, since he gave an excellent, though qualitative, classification of the type of flow obtained at different roughness concentrations and relative roughnesses.

2.6.1 Types of Flow over Rough Boundaries

Morris (1995), classified the flow past a boundary with roughness elements on it into three categories which are Isolated-Roughness Flow, Wake-Interference Type of Flow and Quasi-Smooth Flow. For a graphical view of the following explanations, refer to Figure 19.

In the Isolated Roughness Flow, the wake zone and the vortex generating zone at each roughness element are completely developed and dissipated before the next element is reached. Thus the form drag of each roughness element is practically unaffected by the

presence of the element preceding or succeeding it. It should then be possible to estimate the form drag of the roughness elements if the drag characteristics of a single element in the boundary layer flow are known. The total resistance of the boundary is, under such circumstances, equal to the sum of the form drag and the friction drag on the plan boundary between the roughness elements.

The roughness elements in the Wake Interference Type of Flow are at such a spacing that the separation zones and regions of vortex generation and dissipation behind each element are not fully developed before the next element is met. In other words, the drag coefficient of the roughness element in this case is considerably different from that for a single element.

In the Quasi Smooth Flow, the roughness elements are so close that the flow essentially skims over the crests of the elements and stable vortices exist between the elements. The close spacing of roughnesses leads to a considerable reduction in the form drag coefficient of the roughnesses and consequently the total resistance is greatly reduced.

Morris proposed a criterion for predicting the flow regime and then a method of determining the total resistance of the boundary in all these cases. Not only does the use of these require knowledge of the exact roughness geometry but the relations in several cases were found to predict the resistance poorly. Nevertheless, the classification of flows proposed by Morris does provide a useful insight into the flow over rough surfaces. It should also be noted that the flow past large roughness elements is not truly uniform in the sense that the velocity distributions at different stations along the channel length are not identical. However, the flow may be treated as quasi form, since velocity profiles at stations similarly located with respect to the roughness elements are identical.

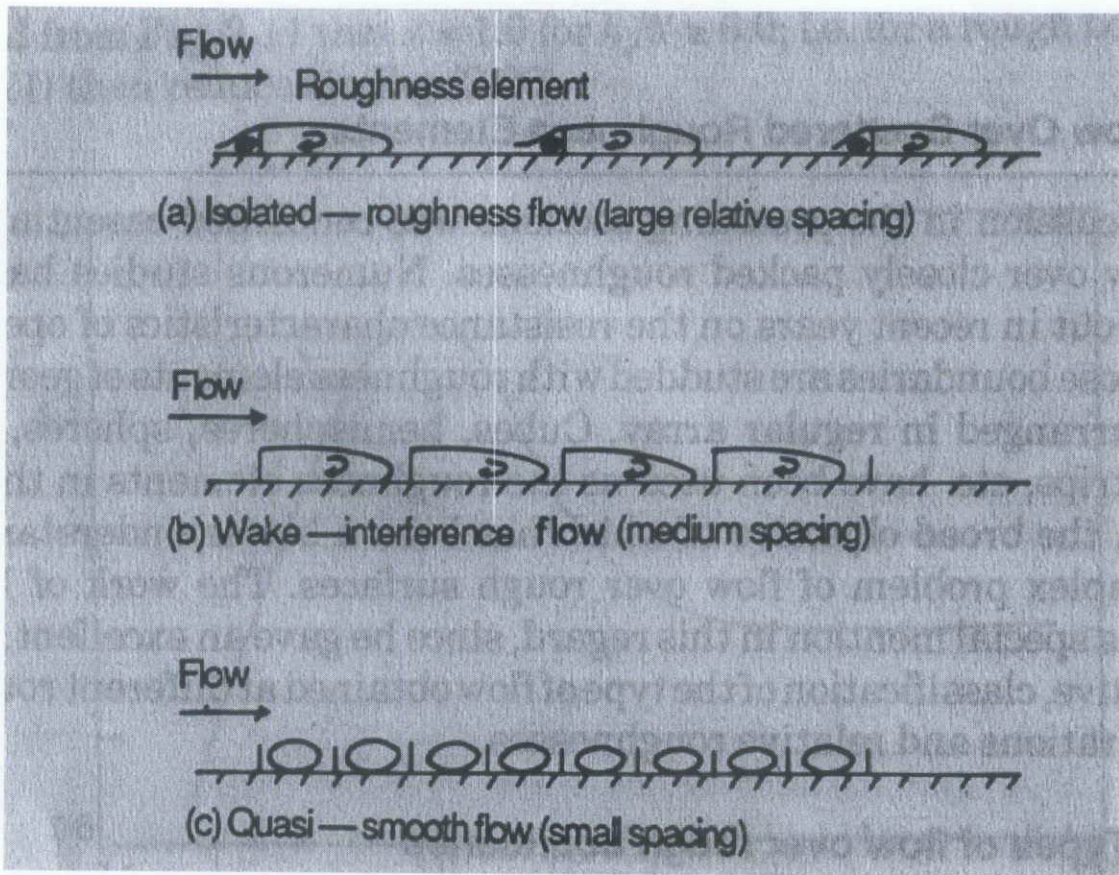


Figure 10 : Classification of flow over scattered roughness (Adapted from Ranga Raju, 2003)

CHAPTER 3

METHODOLOGY

This project involves the evaluation of comparison between data collected for flows going through various rip rap rock designs that have been created. The project will undergo three phases which are extensive literature review on the current use of rip rack rocks structures as well as types of stilling basins, designing of the dam model containing the rip rap rock structure and experimenting with the model using various flows and analyzing the results to compare the effectiveness of the rip rap rock model.

3.1 Tools/Equipments

1. Hydraulics flume
2. Hook and point gauge
3. Current meter
4. Spillway model without rip rap rock
5. Spillway model with rip rap designs (Design Model 1,2 and 3)

3.2 Spillway Model Without Rip Rap

The model of an ogee spillway without rip rap was already available in the lab. The model is made from PVC. The detailed dimensions of the model are 40 cm in length, 30 cm in width and 31 cm in height. A graphical view of the model is shown in Figure 11. This model was used as a reference to compare with the design models that were to be constructed.



Figure 11 : Model of Spillway without Rip Rap

3.3 Spillway Model With Rip Rap Designs

The most important element in this study was the construction and design of the models of spillways which have rip rap designs on them. Among the many designs that were thought of, only three designs were selected for manufacturing. Although the spillway was constructed by a manufacturer, but the construction of the rip rap design was self made. It was done by using mortar as a binder material and limestones as the rip rap for surface roughness. The mortar and limestones were arranged and put in a steel plate which was then slotted onto the spillway model. The steel plate's dimensions are, its width is 30 cm, its length is 15 cm while its height is 1.5 cm.

The size of the spillway was built with respect to the actual Kenyir Dam. Although ideally, a larger scaler model would be required since the spillway at Kenyir is really large, but in order to minimize errors and reduce the scale in this experiment due to the limiting dimensions of the flume, the model was built assuming a ratio of 1:3 with respect to the prototype and only 1/3 parts of the actual spillway is considered in the experiment.

The rip rap designs were constructed with a limiting height of 1 inch because if the height was less than 1 inch, then the water flowing on the structure would not only be effected by surface roughness, as wanted in this experiiment, but also surface tension effects, which is unwanted in this eperiment.

3.3.1 Design Model 1

The first design is taken with reference to the energy dissipator located at the Kenyir Dam. Upon observation, it is noticed that the Kenyir Dam does not have any type of stilling basin at the end of the spillway to dissipate energy. This is due to the fact that the available rocks on site (since it is a rockfill dam) was of good quality and was adequate to dissipate the energy of the water coming down the spillway. Furthermore, since the spillway is seldom used and is situated far away from the dam itself, it did not require the strength provided from the stilling basin. Nevertheless, it would still seem interesting to analyze the amount of energy this design could dissipate, since; after all, it is used in the largest river dam in Malaysia. Figure 15 depicts an actual picture of the Design Model itself after being constructed with an assumed roughness surface of 100%.

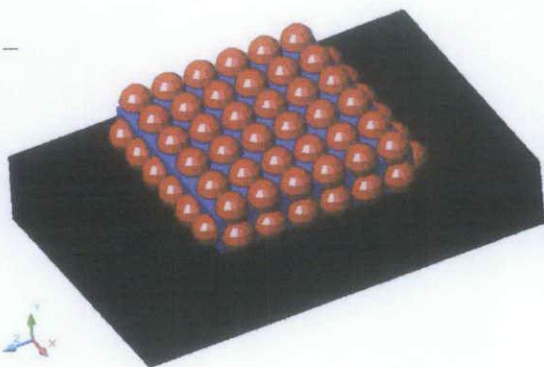


Figure 12 : Design 1: 3D view

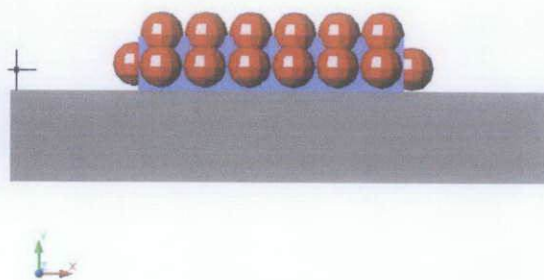


Figure 13 : Design 1 : side view

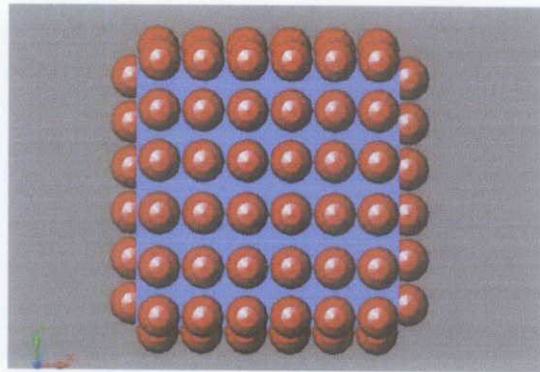


Figure 14 : Design 1 : top view



Figure 15: Plan View of Design Model 1

3.3.2 Design Model 2

This design is slightly similar to the baffle blocks basin design. Baffles are frequently used to aid in formation of the hydraulic jump. Their use can significantly reduce the length of the jump, decrease the required depth for a given discharge condition and provide stability to the jump. Baffle location, size and spacing are the important parameters to be considered in design of a baffle aided stilling basin. Baffle blocks are normally arranged in one or several rows that are orientated perpendicular to the direction of approach flow. The block forces the flow both above and around the obstacles and the

tendency for plunging is thus less. Blocks may be used as terminal elements to deflect remaining bottom currents away from the bed or as baffle blocks, which are impact elements. Figure 19 depicts an actual picture of the Design Model itself after being constructed with calculated surface roughness of 84% compared to Design Model 1.

The general findings of blocks can be summarized as follows:

- The optimum block front face is vertical and perpendicular to the approach flow, the block corners are sharp.
- Usually, one row of blocks is used because the effect of a second row or of staggered block rows is small compared to the first row.

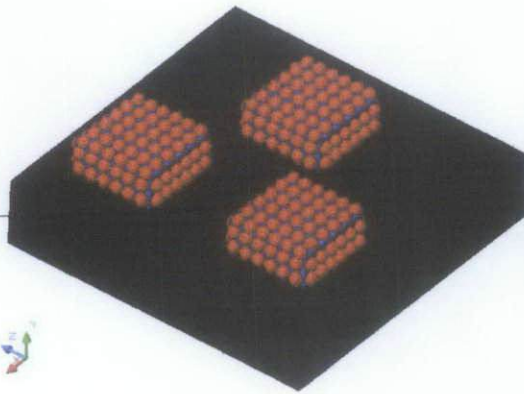


Figure 16 : Design 2 : 3D view

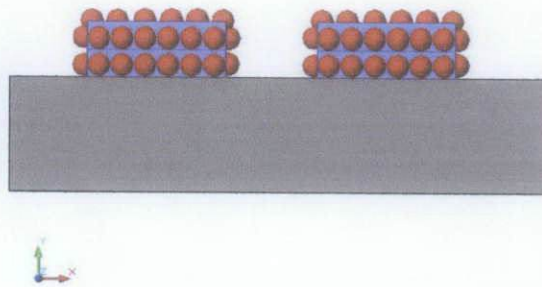


Figure 17 : Design 2 : side view

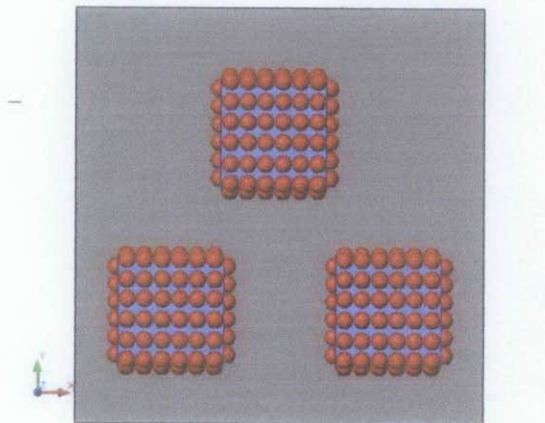


Figure 18 : Design 2 : top view

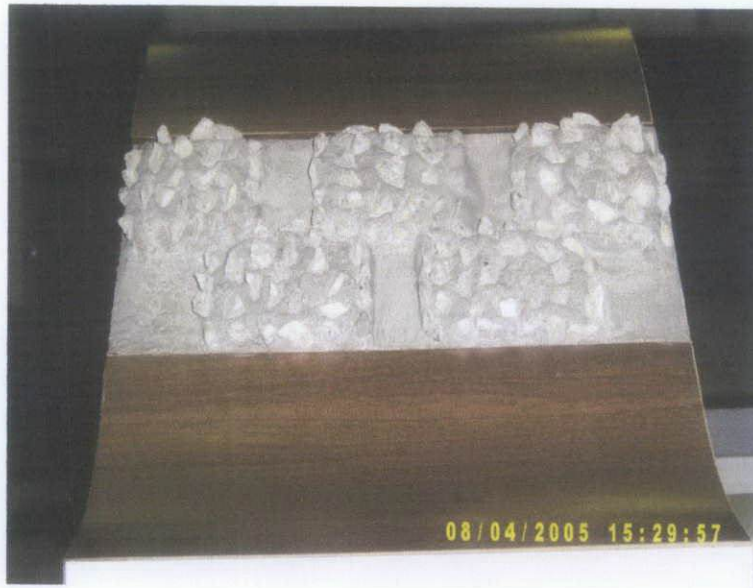


Figure 19: Front View of Design Model 3

3.3.3 Design Model 3

This design is a combination of several designs. On one side, this design was built alike the baffled apron drop. The first systematic study on drops with a baffled apron was presented by Bradley and Peterka (1958). A basic feature of these drops is that they require no tailwater, although the bed scour is reduced if the tailwater forms a pool. The multiple rows of baffle blocks on the chute prevent excessive acceleration of the flow and provide a suitably low terminal velocity, regardless of the height of the drop. In this design, it is understood that as the water has to undergo several paths to reach the downstream, it will endure the multiple rows of baffle blocks and thus energy will be reduced. And as such, as this design is designed utilizing rock structures which are rough in its nature, more energy is thought to be dissipated compared to the usual concrete structures.

On the other side, this design also took into consideration of the gabion designs. The hydraulic performances of gabion stepped chutes are limited by the gabion resistance to

abrasion and destruction, and their safety. Various researches have proposed criteria to prevent the destruction of gabion spillways.

According to Chanson (1994), for gabions laid parallel to the flow, the stability of the gabion revetment depends upon the gabion dimensions and also upon the gap between the gabions. Peyras (1991), advised to design for discharges less than $1 \text{ m}^2/\text{s}$. But Huanxiong and Caiyan (1991), reported large overflow discharges on prototype structures without major damage. For a structure made solely on gabions, the choice of a step slope with skimming flow regime would reduce the number of gabions and the cost of the structure. For an earth fill structure protected by gabions, a flat slope may be more appropriate with the stability required for the embankment. Inclined gabion stepped spillways can also be used. Larger energy dissipation is achieved but their construction requires greater care. A recommended gabion tilt is +5 degrees. Figure 23 depicts an actual picture of the Design Model itself after being constructed with calculated surface roughness of 93% compared to Design Model 1.

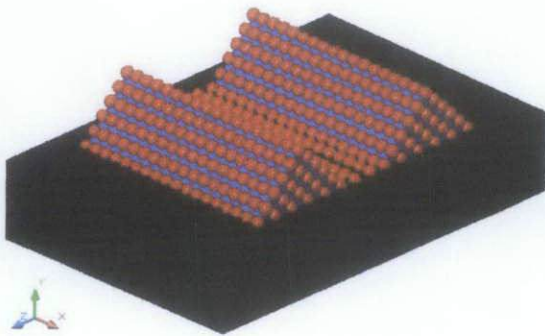


Figure 20 : Design 3 : 3D view

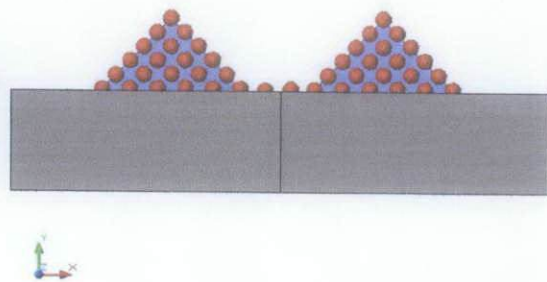


Figure 21: Design 3 : side view

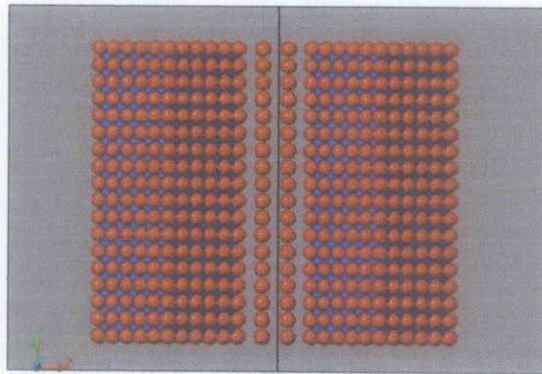


Figure 22 : Design 3 : top view



Figure 23: Front View of Design Model 3

Now, although in these designs, the look of it is not the same to its original design recommended by the various authors, but the concept of these designs are based on the designs of existing hydraulic structures with expectations that these would dissipate energy as well.

3.4 Materials

In this experiment, the vital element, besides the design of the rip rap rock structure is also the type of rock to be used in the design. The rip rap should be angular in shape, hard, and resistant to weathering. Rip rap shall meet the minimum size and gradings in Table 1. The largest stone size shall be 1.5 times the *D50* and the minimum thickness of rip rap shall be 2.5 times the *D50*.

Suggested Minimum Rip-Rap Gradings for Stream Bank Protection.

Class I

Nominal 12 inches diameter or 80 lb. weight. Allowable local velocity up to 10 ft/sec.

Grading Specification:

	100% smaller than 18 inches or	300 lb
at least	20% larger than 14 inches or	150 lb
at least	50% larger than 12 inches or	80 lb
at least	80% larger than 8 inches or	25 lb

Class II

Nominal 20 inches diameter or 400 lb. weight. Allowable local velocity up to 13 ft/sec.

Grading Specification:

	100% smaller than 30 inches or	1500 lb
at least	20% larger than 24 inches or	700 lb
at least	50% larger than 20 inches or	400 lb
at least	80 % larger than 12 inches or	70 lb

Class III

Nominal 30 inch diameter or 1500 lb weight. Allowable local velocity up to 15 ft/sec.

Grading Specification:

	100% smaller than 48 inches or	5000 lb
at least	20% larger than 36 inches or	2500 lb

at least 50% larger than 30 inches or 1500 lb
 at least 80% larger than 20 inches or 400 lb

Note the percentages quoted are by weight; the sizes quote are equivalent spherical diameters, = 1.24 volume

The relative density is assumed to be in the range 2.4 to 2.9.

Water Velocity (feet / second)	Rock D50 (inches)	Rock Weight(pounds)
5	4	3
6	6	10
7	8	24
8	10	47
9	12	81
10	15	158
11	18	273
12	20	375
13	24	650
14	27	925
15	30	1268
16	35	2013

Table 1: Rip rap Minimum D50 Sizing Chart

Although the above table is used for stream bank protection, but it can also be used as reference for this project to create a rip rap rock structure for energy dissipation on a dam. There are many types of rocks that can be used for this purpose such as buff limestone, cocoa rock, gneiss, pink quartz, purple quartz, red limestone, st cloud granite, trap rock. But in this project more focus will be emphasized on the use of granite and limestone since they are the only two type of rocks that are available in abundance at the University Teknologi PETRONAS Civil Engineering Laboratory.



Figure 24 : Red limestone



Figure 25 : Granite

3.5 Experimental Setup

3.5.1 Hydraulics Flume

A flume is an artificial channel used to create flows in the laboratory. It is vital in the progress of this project.



Figure 26 : Existing Flume used in the Experiment

The flume is 10 m long, 45 cm deep and 30 cm wide. The slope of the flume can be adjusted. The transparent sides of the flume are made of hardened glass which is particularly resistant to scratching and abrasion, does not discolor and easy to clean.

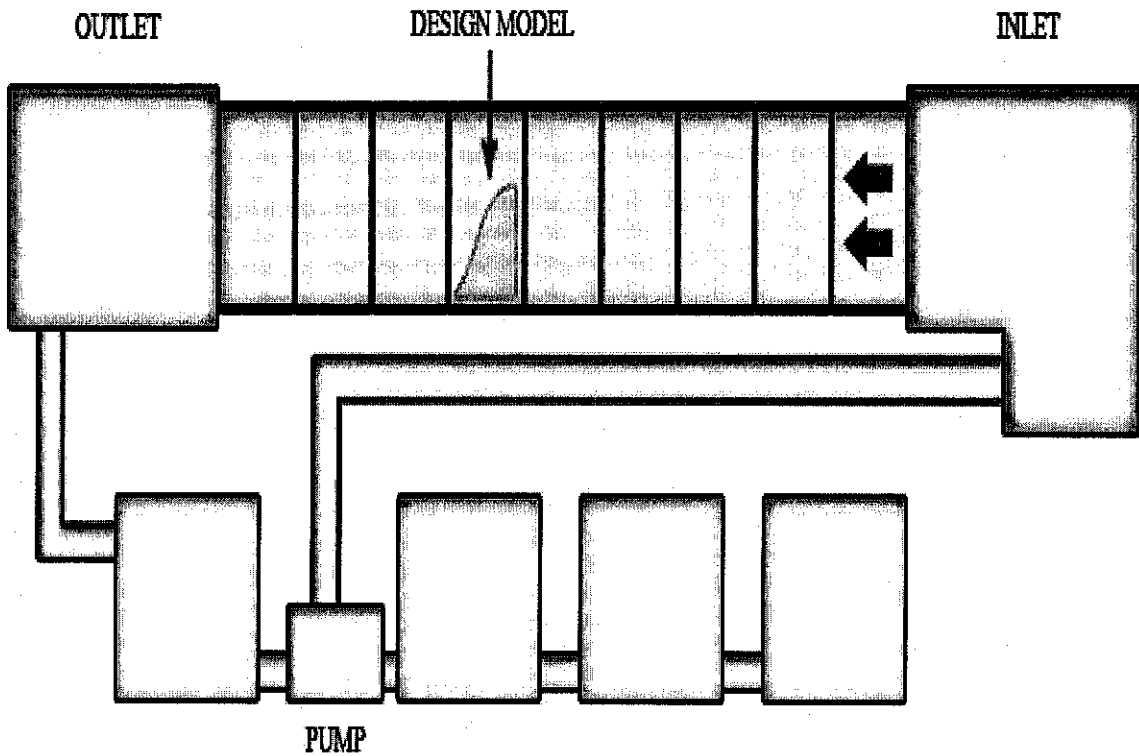


Figure 27 : Experimental Setup of Flume

The prototype of the design is to be put in the flume and various flows is used to go through the energy dissipating structure. As in this stage of the project, the experimental stage has not yet begun, so further explanation on the usage of the flume is yet to be clarified.

3.5.2 Hook and Point Gauge for Modular Flow Channel

The hook and point gauge is used to measure levels and water levels of the flow in the flume. It is possible to carry out measurements over the entire working range of the flow channel, since the measuring point can be traced in the longitudinal direction, across the width and in the depth of the flow cross section.

Point Gauge

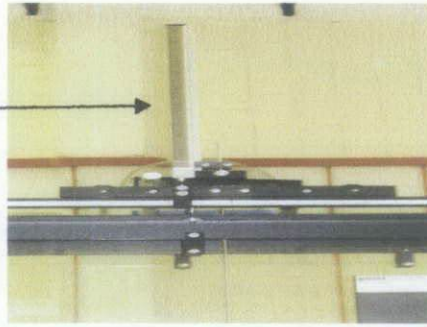


Figure 28: Point Gauge

The water level is measured at two points in the upstream and two points in the downstream section. From these values, further analysis is done in order to establish the energy loss in the stream flow.

3.5.3 *Current Meter*

The current meter (Figure 29) is used to measure the velocity of water at the initial point where the water flows at a steady state. The current meter is a probe which measures the velocity of water by identifying the amount of times the flow of water can turn the probe's propeller. The more amount of times the propeller is turned, thus the larger the reading of velocity will become.



Figure 29: Current Meter

3.6 Experimental Procedures

In order to achieve the objectives of this study, several experiments were performed. The experiment utilized the equipments that were described in the previous section. The procedures are described as follows:

- i) The spillway model's side walls were sealed by inserting the appropriate plastic hoses into the grooves. This was to make sure that the flow would not seep through the grooves and cause error to the flow on the spillway. The spillway was then inserted into the flume.
- ii) The pump was started and the valve was opened to permit water flow into the flume and over the spillway. When a steady flow was established, water depths at different points were measured.
- iii) The measured points were two points at the upstream level (y_{u1} and y_{u2}) and two points at the downstream level (y_{d1} and y_{d2}). Also measured was the depth of water level at a point 3 meters away from the inlet (refer to Figure 30).
- iv) At the point 3 meters away from the inlet, the velocity is measured using the current meter.
- v) The same procedures from step (i) to step (iv) is repeated for different flowrates where each flowrate indicated by the flowmeter is taken note.
- vi) Procedures from step (i) to (v) is repeated for all design models.
- vii) All the data taken during the experiments are presented in table 2, 3, 4 and 5 in the Appendix.

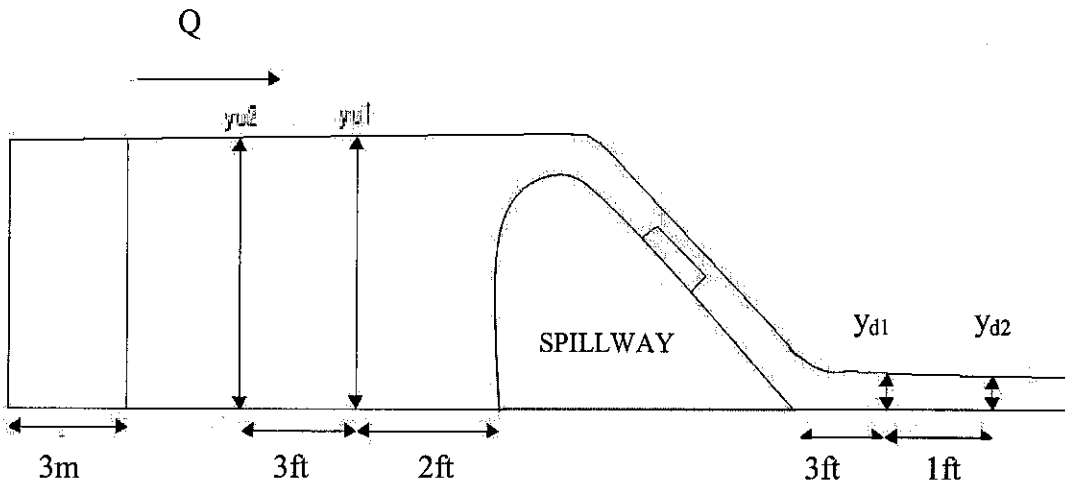


Figure 30: Points of Water Depth Measurements in the Flume

CHAPTER 4

RESULTS AND DISCUSSION

This part of the report explains of the results of the experiments that have been carried out in the identification of the most effective energy dissipator. The experimental results were analyzed and graphically presented in this chapter. The data which led to the graphs can be referred to in the Appendix section.

This chapter is divided into four parts which are discussions on water depth computation at upstream and downstream sections, discrepancy between theoretical and actual flowrate, energy loss and the observations made during the experiment.

4.1 Water Depth Computation

In the procedure for this experiment, one of the key steps was taking the readings of water level at the upstream and downstream section. Two points were selected at the upstream section, y_{u1} and y_{u2} , and another two points at the downstream section, y_{d1} and y_{d2} as reference points for these measurements.

4.1.1 Upstream Section

Referring to the results in Table 2, 3, 4 and 5 in the Appendix, it is observed that the depth of water in the upstream section, y_{u1} and y_{u2} have values of almost the same where the differences between the values of two sections was in the range of 0.1% to 0.9%. The difference is relatively small because the water is tranquil and there is no disturbance. Thus the average of y_{u1} and y_{u2} is selected for the computation of energy loss at the upstream section.

4.1.2 Downstream Section

Referring to the results in Table 2, 3, 4 and 5 in the Appendix, it is observed that in certain cases, the depth of water at the downstream section y_{d1} and y_{d2} had values that were different from each other where the range of difference between the values of the two sections were in the range of 1% to 59%. The values varied larger because especially when the flowrate was increased. This was because as the flowrate increased, the flow became turbulent. When this occurred it was difficult to obtain a precise measurement of water depth due to the fluctuations of water level. Ideally, it would be recommended to obtain the reading of water depth at points where the flow of water is stable. But in this experiment, it was impossible to do so, because if the reading was taken further downstream, away from the spillway, the water flow at that point would have undergone friction loss as well and if that occurred, thus the objective of this experiment would not have been achieved properly. So that is why, eventhough the water flow is turbulent at the points that were selected for measurement, the reasons for doing so was so that the

measurements at those points could be done without the influence of friction loss. Nevertheless, to reduce the amount of error, the average depth of the points was used in the computation of energy loss.

4.2 Theoretical Flowrate, Q_t and Actual Flowrate, Q_a

In this study, the theoretical flowrate, Q_t refers to computed flowrate which is flowrate that was established based on the measurement of velocity performed in the experiment by using the current meter. Meanwhile, the actual flowrate, Q_a was obtained from the flow meter which was attached to the flume in the laboratory. The reason that there are two flowrates used in this experiment is because Q_a depicted by the flow meter readings in the laboratory was found to be unreliable due to its instability. The reading of the flume flowmeter seemed to variate and did not point to one particular value at a specific time. Thus the reading obtained from the meter was just used as a basis of reference for this experiment, whilst Q_t was used in the calculations of energy loss.

In figure 36, there are two plots where one refers to the desired values of Q_a and Q_t while the other line refers to the experimented values of Q_a and Q_t that were obtained and used in this experiment. Theoretically, it is always desired to have values of Q_a and Q_t that are equal to each other, but it is just impossible to have so in this experiment because of the fluctuations of the flow meter which was attached to the flume in the laboratory,

In the first two low flowrates, the plots of the experimented values Q_a and Q_t did not vary much from the desired values of Q_a and Q_t . This is reasonable because when the flowrates were low, the pump did not fluctuate much, resulting in more stable readings to be obtained. However as the flowrates increased, it is seen from the figure that the values of the experimented values of Q_a and Q_t seemed to move further away from the desired values of Q_a and Q_t . And since the graph of experimented values of Q_t and Q_a looked to be below the line of the desired values of Q_a and Q_t , thus proving that Q_t seemed to be relatively higher than Q_a . This is reasonable because as flowrate increases, the water in

the flume begins to become more turbulent. Turbulent flow results in more losses to the flow and thus that is why the actual flowrate is lower than the theoretical flowrate as the experiment is performed using higher flowrates.

Therefore, only Q_t is used in the computation of energy loss.

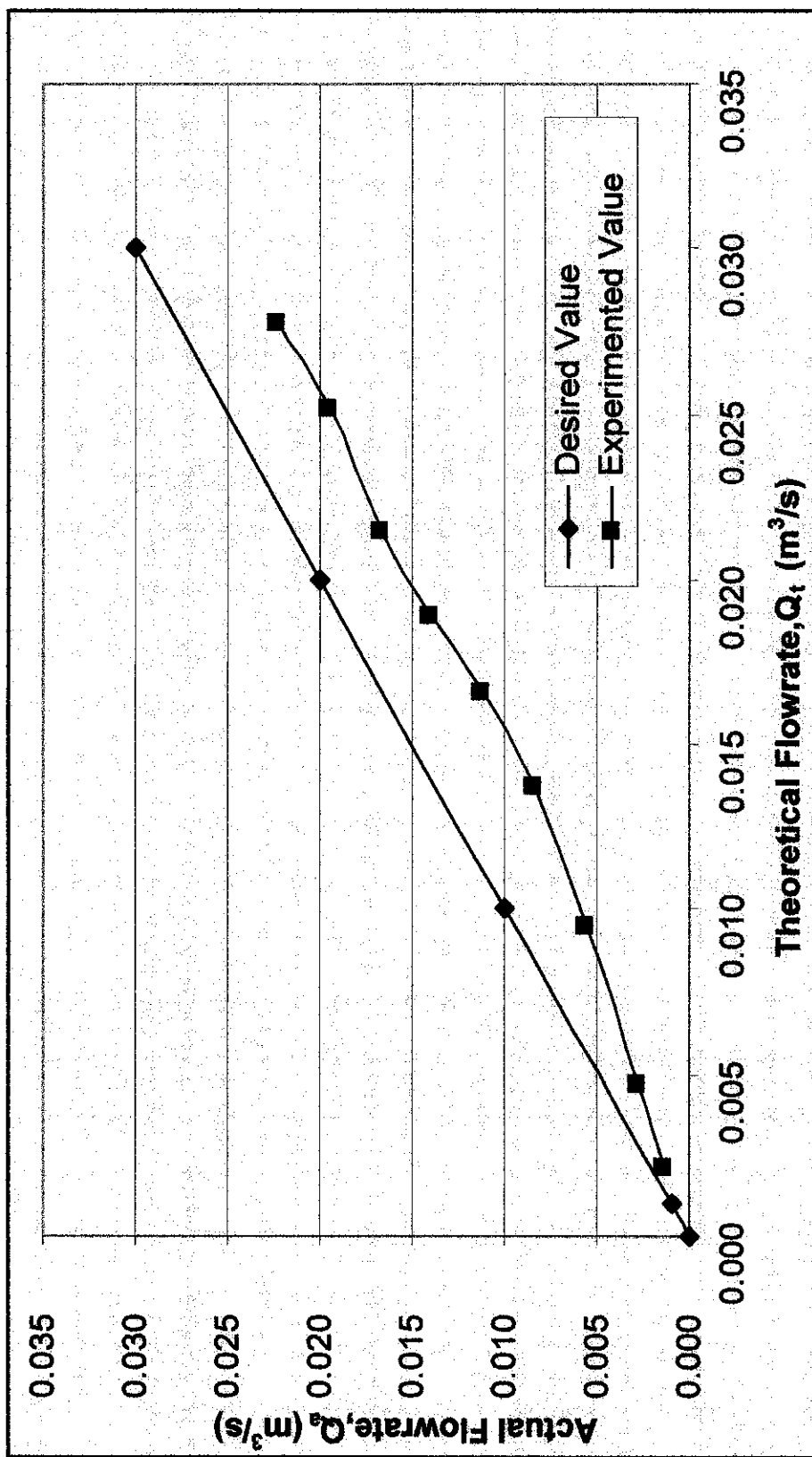


Figure 31: Comparison Between the Theoretical and Actual Flowrate

4.3 Energy Loss

The main concern in this experiment is the energy loss. The main objective of this experiment is to measure the effectiveness of the rip rap rock designs by identifying which model can dissipate most energy based on the experiments performed in the flume. The main equation used to calculate the energy loss achieved by each experiment is the modified energy equation as given by equation 4 earlier.

Figure 32 depicts a graph showing the characteristics of four types of designs that went through the experiment in the flume. The four designs are as follows, a model of a spillway without rip rap rock, Design Model 1, Design Model 2, and Design Model 3. From the figure, the characteristics of each design model that was experimented upon can be identified.

Firstly, it is observed that for the experiment of the spillway without rip rap, the energy loss decreases as the flowrate increases. This was expected, because for this experiment, no energy dissipator is located on the spillway thus providing a smooth flow on the spillway as the flowrate increases. This is why, as the flow increases, the energy loss becomes lower and lower. The experiment with this model was done to identify the fact on whether or not the rip rap rock energy dissipator would prove to be effective. And so, as observed from the graph, the other models managed to dissipate more energy compared to this particular model, thus proving that the installation of the rip rap rock succeeded in fulfilling its objective which was to dissipate energy.

The next objective is to identify which model could dissipate most energy thus proving to be the most effective design among the three design models that were created and experimented upon. From the graph, it is observed that the energy loss was greatest for Design Model 1, as flowrate increased with a range of 1% to 251%. This was quite a surprise because initially, it was predicted that Design Model 3 would achieve most energy loss since its model was designed based on several designs of energy dissipator. On one side it was designed alike the baffled apron drop and on the other side, it was also

designed alike the gabion designs. Astonishingly, the predicted outcome did not occur as the results of the experiments show from the graph, Design Model 1 revealed the most amount of energy loss. Thus it is concluded that among all designs, the Design Model 1 is identified as the most effective energy dissipator as it is capable of dissipating the most amount of energy compared to the other models. The reason why this structure was identified as the most effective energy dissipator is mostly because, among all design models, this structure had the largest area of surface roughness. It had rip rap rocks covering the entire area provided. Furthermore, it had the most number of rocks attached to it. Therefore, it is assumed that the roughness surface area of Design Model 1 is 100%. Another point that should be highlighted here is the fact that Design Model 1 was designed with reference to the energy dissipator located at the spillway of the Kenyir Dam. The design did not have a specific rock structure as the rocks were randomly arranged on a flat surface. But since Kenyir Dam uses the design, and the experiment performed revealed that the particular design dissipated most amount of energy, thus the design used in Kenyir Dam is justified by the results of this experiment. Figure 33 depicts flow variations of Design Model 1.

Initially, Design Model 3 was expected to be the most effective energy dissipator, but upon observation of the figure 35, it was observed that the amount of energy loss for this design decreased as flowrate increased with a range of 0.1% to 215%. Upon closer observation during the experiment, refer to Figure 35 the flow hit the first stepped structure and lost some energy but then before it reached the second step, there was a gap in between the two steps which did not have any rip rap thus no surface roughness and thus this may be the reason why this design failed to dissipate more energy. Due to this gap, the water managed to flow freely without any interference for some time before reaching the second step. In terms of total area of surface roughness, this design had less amount of surface roughness compared to Design Model 1. The surface roughness area of Design Model 3 is 93% compared to Design Model 1.

Design Model 2 was also expected to dissipate more energy compared to Design Model 1. This was because this design was based on the baffle blocks design. But based on the

Figure 32, it is observed that the energy loss for this design also decreased as flowrate increased with a range of 1% to 38%. Figure 34 shows a simple description of how the flow of water went through this design. It is noticed that there are three blocks of rip rap in the first row and two blocks of rip rap on the second row. One reason why this design failed to dissipate more energy is because the blocks had gaps between them thus somehow allowing part of the water to flow freely between the blocks of rip rap. Thus this probably proves why this design did not manage to dissipate as much energy as expected. In terms of surface area, this design had less surface roughness compared to Design Model 1. The surface roughness area of Design Model 2 is 84% compared to Design Model 1.

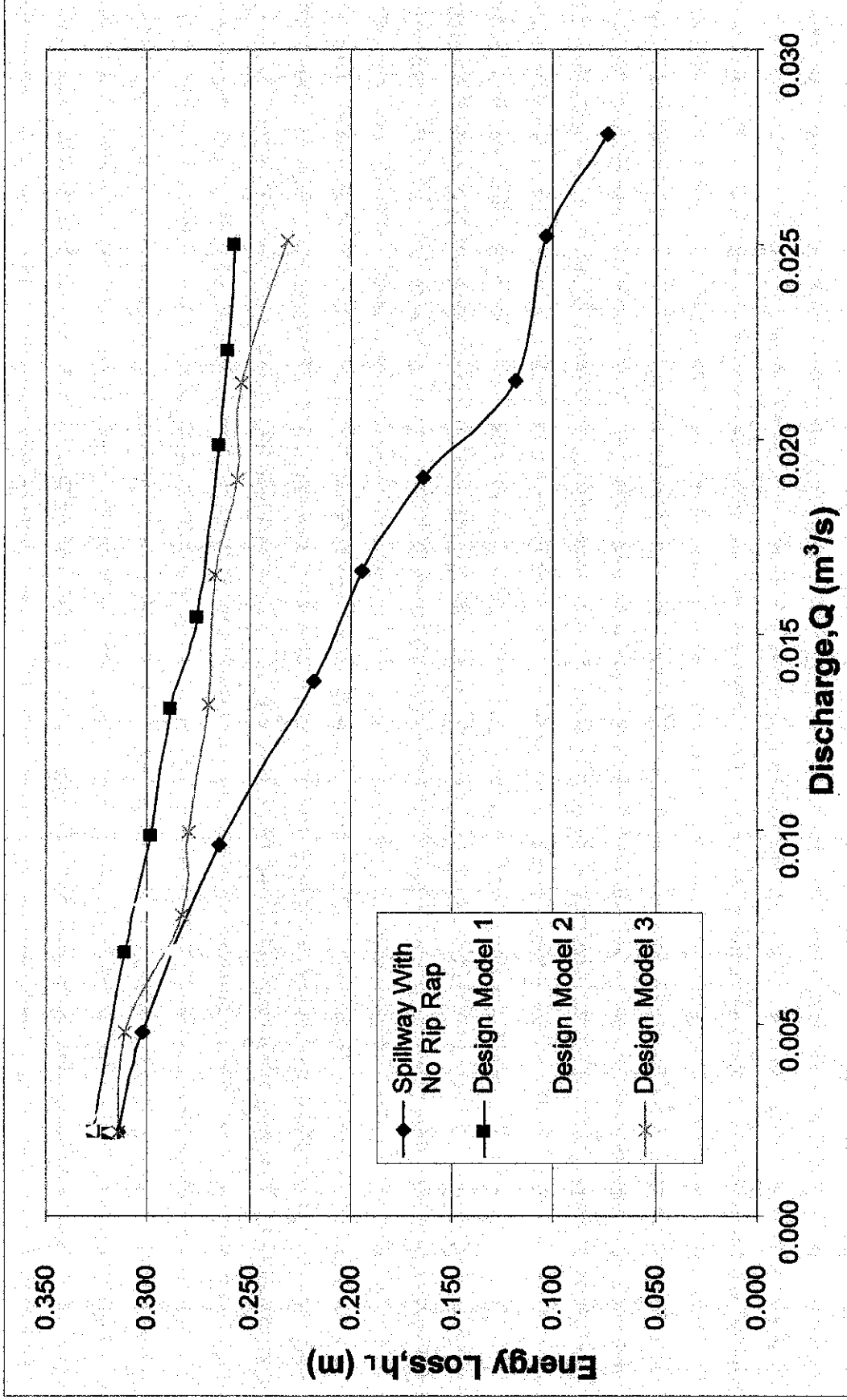


Figure 32: Graph of Energy Loss versus Theoretical Discharge for All Models

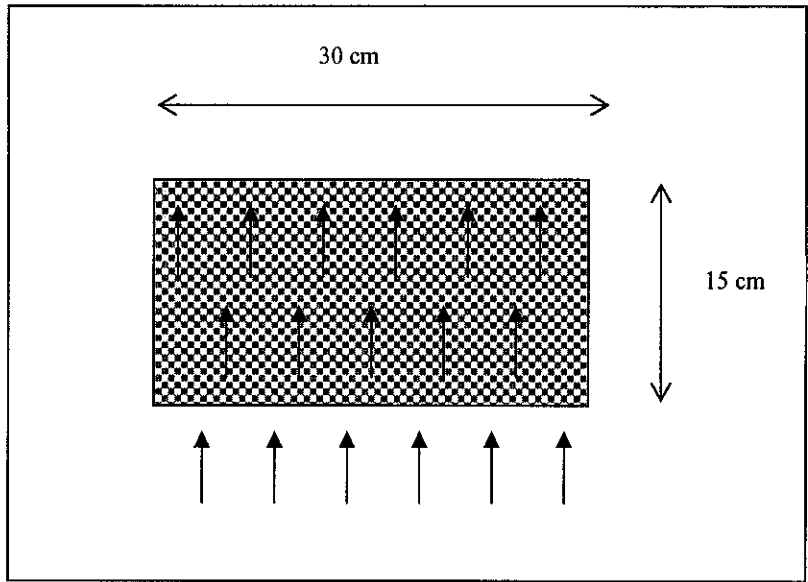


Figure 33: Flow Variations on Design Model 1

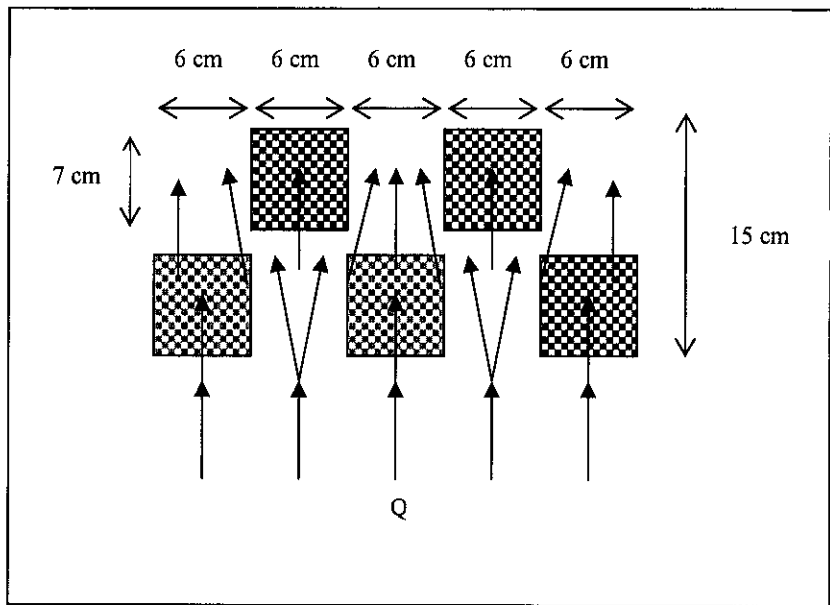


Figure 34: Flow Variations on Design Model 2

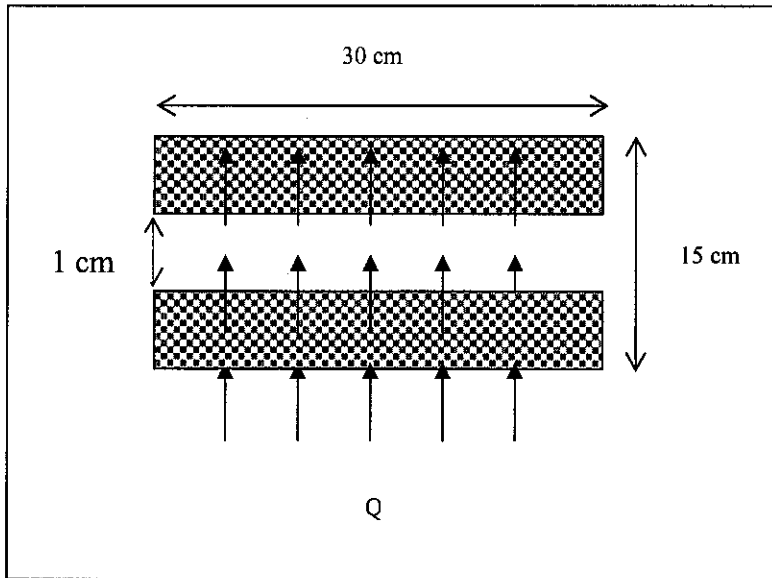


Figure 35: Flow Variations on Design Model 3

4.4 Observations

Following are several observations made during the experiment based on situations with different flowrates.

4.4.1 Design Model 2

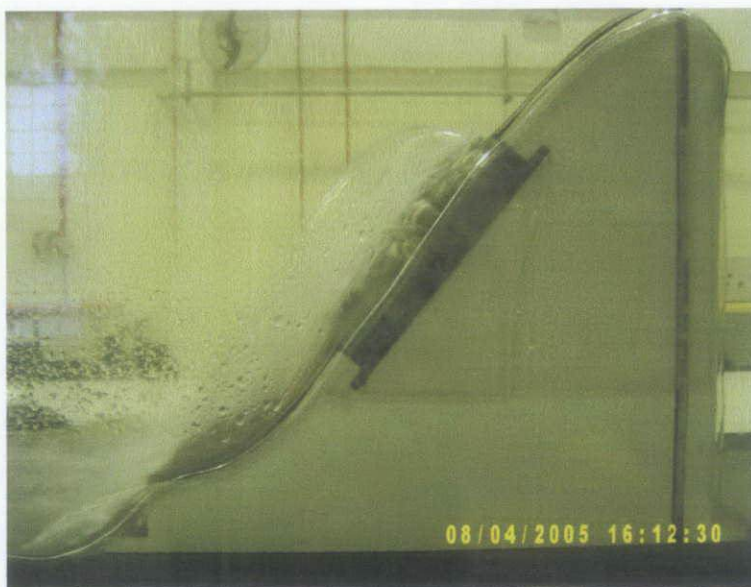


Figure 36: Side view of Design Model 2 at 5 m³/hr

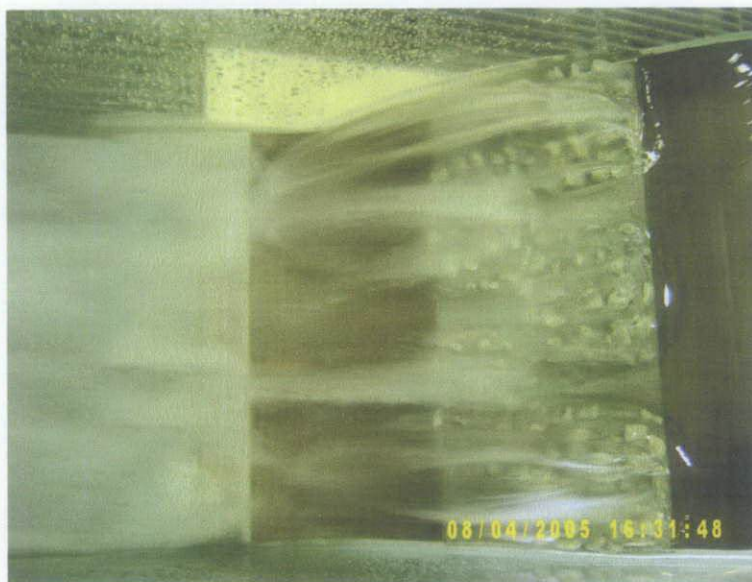


Figure 37: Plan view of Design Model 2 at 5 m³/hr

Figure 36 and 37 shows flow of water at 5 m³/hr. It is observed that part of the water is diverted by the initial rip rap block and thus creates a jump. The flow jumps over the

block and immediately flows downstream. This is probably why at this point of the experiment, the energy loss was great (refer to figure 35). The energy loss occurred mostly due to the jump rather than the surface roughness. Referring to Figure 36, the design managed to divert the water to a distance of 28 cm.



Figure 38: Side view of Design Model 2 at 80 m³/hr

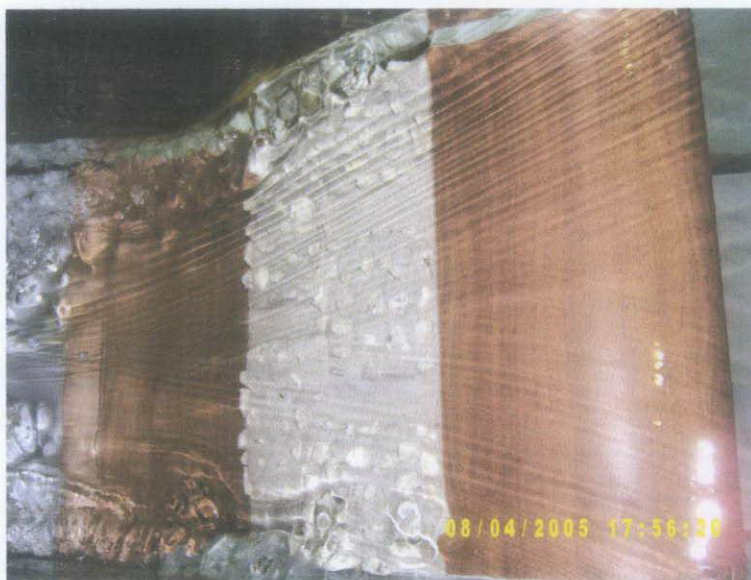


Figure 39: Plan view of Design Model 2 at 80 m³/hr

Figure 38 and 39 shows flowrate at $80 \text{ m}^3/\text{hr}$. Upon observation from the side view of the model, the water level is high on the structure due to the high flowrate with a depth of 28 cm. Thus there are no more jumps over the block as initially occurred during the low flow. Referring to the top view of the model, it is observed that the flow of water is as such depicted by Figure 34. Thus showing that for this model, the flow of water was not just flowing on the blocks of rip rap, but also finding ways to flow in between the gaps of the rip rap blocks thus evading any sort of energy loss due to surface roughness. Thus, proving why this design did not manage to dissipate much energy compared to Design Model 1.



Figure 40: Side view of Downstream at $5 \text{ m}^3/\text{hr}$

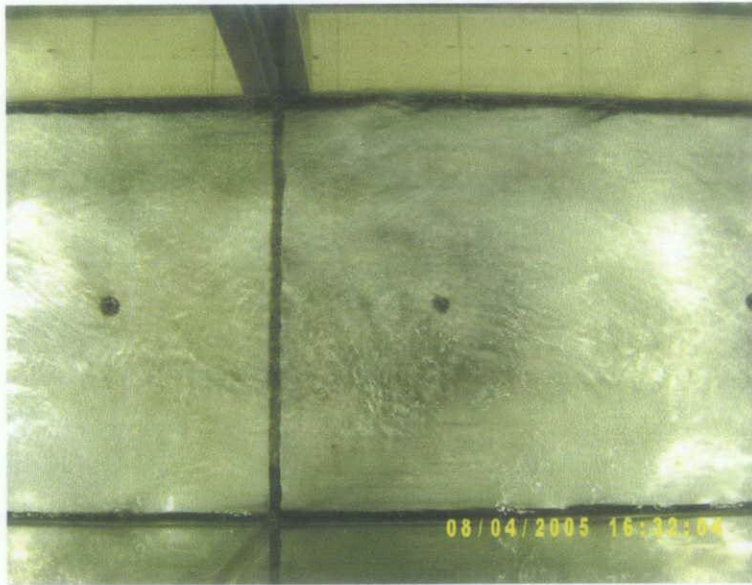


Figure 41: Plan view of Downstream at 5 m³/hr

Figure 40 and 41 depicts flow downstream section at 5 m³/hr. The figure shows that at low flow, the flow was tranquil and there was not much disturbance to the water profile. Thus it was easier to obtain the water depth at y_{d1} and y_{d2} due to the water elevations not varying as much with a range of 10% difference from each other (refer to Table 5).

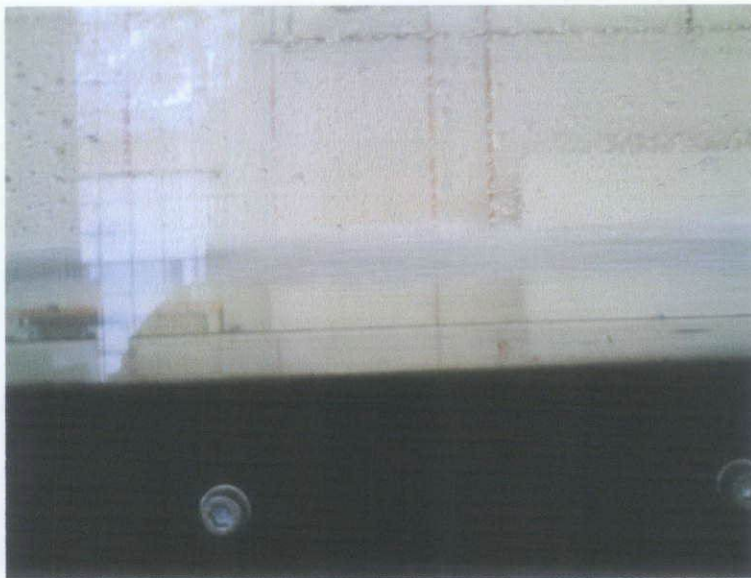


Figure 42: Side view of Downstream at 80 m³/hr



Figure 43: Plan view of Downstream at 80 m³/hr

Figure 42 and 43 depicts flow at downstream section at 80 m³/hr. The figure shows that at large velocity, the flow of water was turbulent and it was difficult to obtain a correct reading of y_{d1} and y_{d2} . Thus that is why the variations between the values of y_{d1} and y_{d2} were large with a range of 24% difference from each other (refer to Table 5). In order to overcome this error, the average value of y_{d1} and y_{d2} was used in the calculation of energy loss.

4.4.2 Design Model 3

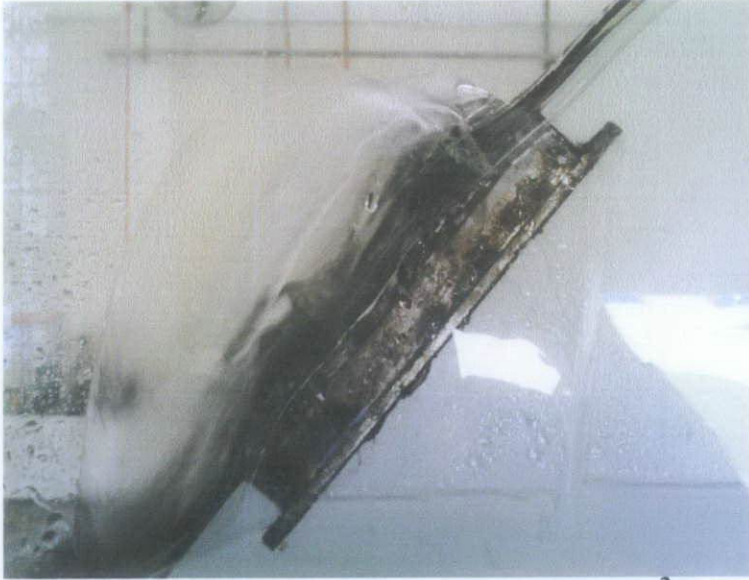


Figure 44: Side view of Design Model 3 at 5 m³/hr



Figure 45: Plan view of Design Model 2 at 5 m³/hr

Figure 44 and 45 shows flow of water at 5 m³/hr. It is observed that part of the water is diverted by the initial steps of rip rap and thus creates a jump. The flow jumps over the first row of steps and immediately flows downstream. This is probably why at this point of the experiment, the energy loss was great (refer to figure 35). The energy loss occurred mostly due to the jump rather than the surface roughness. Referring to Figure 44, the

design managed to divert the water to a distance of 29 cm which is more than the distance diverted by Design Model 2.

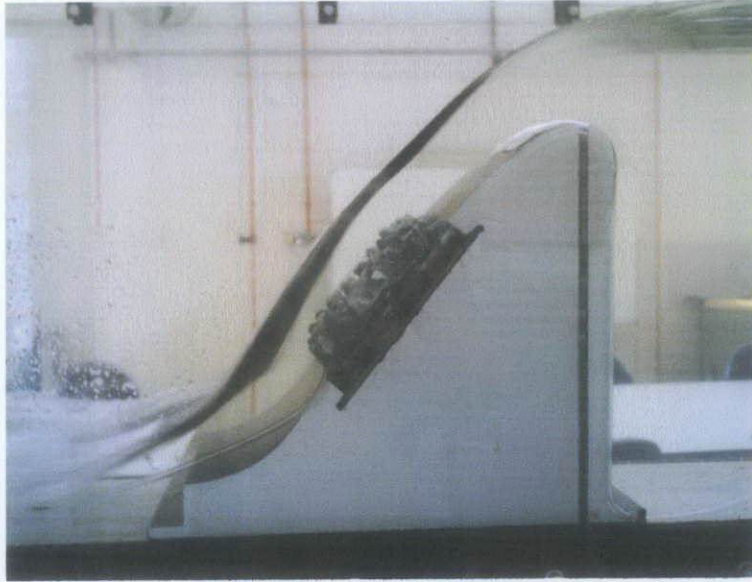


Figure 46: Side view of Design Model 2 at 80 m³/hr

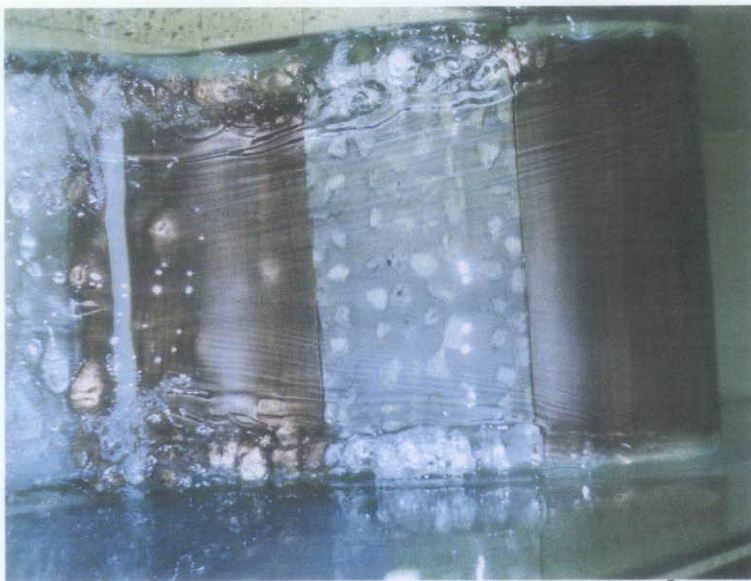


Figure 47: Plan view of Design Model 2 at 80 m³/hr

Figure 46 and 47 shows flowrate at 80 m³/hr. Upon observation from the side view of the model, the water level is high on the structure due to the high flowrate with a depth of 29 cm. This value is less than the water depth at Design Model 2 at this similar stage. Also, there are no more jumps over the block as initially occurred during the low flow.

Referring to the top view of the model, it is observed that the flow of water is as such depicted by Figure 35 thus showing that for this model, the flow of water hit the first stepped structure and lost some energy but then before it reached the second step, there was a gap in between the two steps which did not have any rip rap thus no surface roughness and thus this may be the reason why this design failed to dissipate more energy. Due to this gap, the water managed to flow freely without any interference for some time before reaching the second step. In terms of total area of surface roughness, this design had less amount of surface roughness compared to Design Model 1.



Figure 48: Side view of Downstream at 5 m³/hr

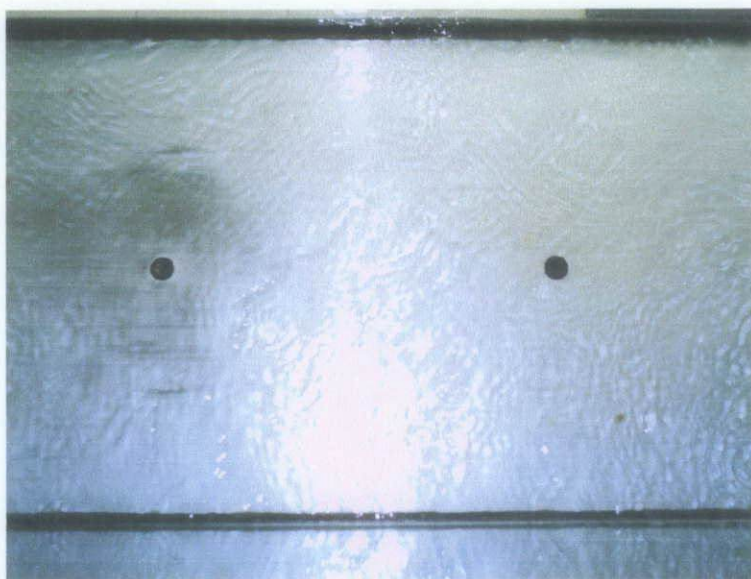


Figure 49: Plan view of Downstream at 5 m³/hr

Figure 48 and 49 depicts flow downstream section at $5 \text{ m}^3/\text{hr}$. The figure shows that at low flow, the flow was tranquil and there was not much disturbance to the water profile. Thus it was easier to obtain the water depth at y_{d1} and y_{d2} due to the water elevations not varying as much with a range of 4% difference from each other (refer to Table 5).

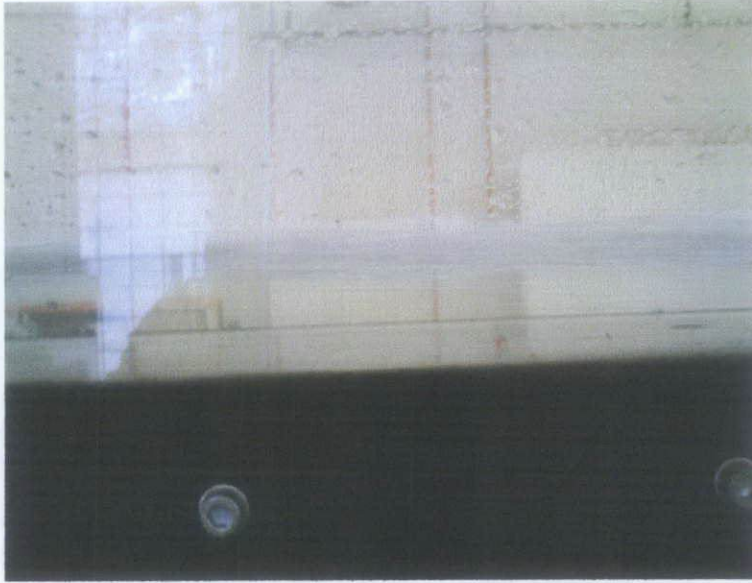


Figure 50: Side View of Downstream at $80 \text{ m}^3/\text{hr}$



Figure 51: Plan View of Downstream at $80 \text{ m}^3/\text{hr}$

Figure 50 and 51 depicts flow at downstream section at $80 \text{ m}^3/\text{hr}$. The figure shows that at large velocity, the flow of water was turbulent and it was difficult to obtain a correct

reading of y_{d1} and y_{d2} . Thus that is why the variations between the values of y_{d1} and y_{d2} were large with a range of 11% difference from each other (refer to Table 5). In order to overcome this error, the average value of y_{d1} and y_{d2} was used in the calculation of energy loss.

CONCLUSION

It can be concluded that this project has reached its final goal which is in identifying the most effective design of rip rap rock energy dissipator. In this study, in depth investigation was done to determine the exact formation of rip rap. Based on the many available designs, three designs were chosen for modeling and were manufactured. After analyzing the results from the experiment and comparing their graphical behaviour, it is identified that Design Model 1 which was designed with reference to the design of the energy dissipator located at the Kenyir Dam, Terengganu, proved to be the one to dissipate most energy and thus is the most effective energy dissipator. Thus, the reasoning for the type of design of the energy dissipator at the Kenyir Dam is justified with the results of this experiment. Based on the three design models that were experimented upon, it seemed that the most important parameter which influenced the amount of energy dissipated was the amount of surface roughness. Design Model 1 which dissipated most energy had a surface roughness of 100% followed by Design Model 3 with 93% and Design Model 2 with 84%.

REFERENCES

- American Society of Civil Engineers. (1995). "*Hydraulic Design of Spillways*". ASCE Press. 120p.
- Chadwick, A. and Morfett, J. (2002). "*Hydraulics in Civil Engineering and Environmental Engineering*". Spon Press. 600p.
- Chanson, H. (1994). "*Hydraulic Design of Stepped Cascades, Channels, Weirs and Spillways*". Pergamon. 261p.
- Mays, L. W. (2001). "*Water Resources Engineering*". John Wiley & Sons, Inc. 761p.
- Minor, H. E. and Hager Q. H. (2000). "*Hydraulics of Stepped Spillways*". A.A. Balkema/Rotterdam/Brookfield, 201p.
- Montes, S. (1998). "*Hydraulics of Open Channel Flow*" ASCE Press. 384p.
- Novak, P., Moffat, A. I., Nalluri, C. and Narayanan, R. (1997). "*Hydraulic Structures*". Second Edition, E & FN Spon, Chapman & Hall. 532p.
- Ranga Raju, K. G. (2003). "*Flow Through Open Channels*". Tata McGraw Hill Publishing Company Limited. 428p.
- Smith, C.D., Professor Of Civil Engineering, University of Saskatchewan. (1995). "*Hydraulic Structures*". 11-24p.
- Vischer, D. L. and Hager, W. H. (1995). "*Energy Dissipators*". A.A. Balkema/Rotterdam/Brookfield. 201p.

Table 2: Results of Experiment with Spillway without Rip RapActual Flowrate, Q_a

Q_1 (m ³ /hr)	Q_2 (m ³ /hr)	Q_3 (m ³ /hr)	Q_{ave} (m ³ /hr)	Q_{ave} (m ³ /s)
5.02490	5.09340	5.01720	5.04517	0.001401
10.03600	10.02000	10.06600	10.04067	0.002789
20.11800	20.18900	20.09900	20.13533	0.005593
30.13200	30.25500	30.17100	30.18600	0.008385
40.78700	40.61300	40.56000	40.65333	0.011293
50.11100	50.57800	50.41300	50.36733	0.013991
60.02100	60.23400	60.07100	60.10867	0.016697
70.24300	70.17400	70.61600	70.34433	0.01954
80.57400	80.21000	80.03000	80.27133	0.022298

Theoretical Flowrate, Q_t

Y_o (cm)	V at $0.5Y_o$ (cm/s)	Q at $0.5Y_o$ (m ³ /s)
34.50000	2.10000	0.00217
35.50000	4.50000	0.00479
37.20000	8.60000	0.00960
38.60000	11.90000	0.01378
40.80000	13.60000	0.01665
41.70000	15.20000	0.01902
42.50000	16.90000	0.02155
43.30000	19.40000	0.02520
44.20000	21.00000	0.02785

Water Depth at Upstream and Downstream Section

y_{u1} (cm)	y_{u2} (cm)	$y_{u(average)}$ (cm)	y_{d1} (cm)	y_{d2} (cm)	$y_{d(average)}$ (cm)
34.00000	34.20000	34.10000	2.10000	1.90000	2.00000
35.40000	35.50000	35.45000	2.10000	1.40000	1.75000
37.20000	37.20000	37.20000	2.20000	1.70000	1.95000
38.60000	38.70000	38.65000	3.30000	2.20000	2.75000
39.80000	39.70000	39.75000	3.60000	2.40000	3.00000
41.30000	41.40000	41.35000	3.80000	1.90000	2.85000
42.10000	42.30000	42.20000	4.00000	2.20000	3.10000
42.80000	43.10000	42.95000	4.40000	2.60000	3.50000
43.50000	43.90000	43.70000	4.60000	2.70000	3.65000

Energy loss Between Upstream and Downstream

$y_{u(average)}$ (cm)	V upstream (m/s)	E upstream (m)	$y_{d(average)}$ (cm)	V downstream (m/s)	E downstream (m)	E loss (m)
34.10000	1.90000	0.341104	2.00000	0.37154	0.02654	0.31457
35.45000	0.08600	0.354877	1.75000	0.79875	0.05252	0.30236
37.20000	0.11885	0.37272	1.95000	1.27968	0.10846	0.26426
38.65000	0.13959	0.387493	2.75000	1.67033	0.16970	0.21779
39.75000	0.15329	0.398698	3.00000	1.84960	0.20436	0.19433
41.35000	0.17020	0.414976	2.85000	2.07816	0.25062	0.16436
42.20000	0.19558	0.42395	3.10000	2.31694	0.30461	0.11934
42.95000	0.21240	0.431799	3.50000	2.40006	0.32859	0.10321
43.70000	0.21243	0.4393	3.65000	2.54301	0.36611	0.07319

Table 3: Results of Experiment with Design Model 1**Actual Flowrate, Q_a**

Q_1 (m ³ /hr)	Q_2 (m ³ /hr)	Q_3 (m ³ /hr)	Q_{ave} (m ³ /hr)	Q_{ave} (m ³ /s)
5.0549	5.0212	5.0936	5.05667	0.00141
10.086	10.123	10.039	10.0827	0.00280
20.039	20.145	20.013	20.0657	0.00557
30.026	30.042	30.072	30.0467	0.00835
40.097	40.016	40.011	40.0133	0.01111
50.093	50.0058	50.085	50.0613	0.01390
60.035	60.047	60.162	60.0813	0.01669
70.039	70.013	70.024	70.0253	0.00195
80.093	80.015	80.028	80.0453	0.02223

Theoretical Flowrate, Q_t

Y_o (cm)	V at $0.5Y_o$ (cm/s)	Q_{ave} (m ³ /s)
34.6	2.1	0.00141
35.5	2.1	0.00280
37	6.2	0.00557
38.3	8.6	0.00835
39.5	11.1	0.01111
40.4	12.8	0.01390
41.2	16.1	0.01669
42.1	17.7	0.00195
43	19.4	0.02223

Water Depth at Upstream and Downstream Section

y_{u1} (cm)	y_{u2} (cm)	$y_{u(average)}$ (cm)	y_{d1} (cm)	y_{d2} (cm)	$Y_{d(average)}$ (cm)
34.6	34.6	34.6	1.0	1.1	1.1
35.5	35.5	35.5	1.5	1.2	1.2
37.2	37.2	37.2	1.6	1.7	1.7
38.3	38.3	38.3	1.8	2.2	2.2
39.5	39.5	39.5	2.2	2.4	2.4
40.5	40.5	40.5	2.5	2.6	2.6
41.3	41.3	41.3	2.8	3.0	3.0
42.1	42	42.05	3.3	3.4	3.4
43	42.8	42.9	3.5	3.5	3.5

Energy loss Between Upstream and Downstream

$y_{u(average)}$ (cm)	V upstream (m/s)	E upstream (m)	$Y_{d(average)}$ (cm)	V downstream (m/s)	E downstream (m)	E loss (m)
34.6	0.02100193	0.34602248	1.1	0.32296296	0.02781626	0.31820622
35.5	0.02103286	0.35502255	1.2	0.31111111	0.02893324	0.32608931
37.2	0.06164875	0.37219371	1.7	0.7908046	0.06087421	0.3113195
38.3	0.08598782	0.38337686	2.2	1.01333333	0.08483662	0.29854024
39.5	0.11097046	0.39562765	2.4	1.16888889	0.10713819	0.28848946
40.5	0.12765432	0.40583056	2.6	1.34285714	0.13040955	0.27542102
41.3	0.16053269	0.41431349	3.0	1.42580645	0.15011488	0.26419861
42.05	0.17717004	0.42209986	3.4	1.47524752	0.16142534	0.26067451
42.9	0.19448329	0.43092782	3.5	1.53088685	0.17395028	0.25697753

Table 4: Results of Experiment with Design Model 2Actual Flowrate, Q_a

Q_1 (m ³ /hr)	Q_2 (m ³ /hr)	Q_3 (m ³ /hr)	Q_{ave} (m ³ /hr)	Q_{ave} (m ³ /s)
5.0802	5.0705	5.0300	5.06023	0.001406
10.086	10.123	10.039	10.08267	0.002801
20.039	20.145	20.013	20.06567	0.005574
30.026	30.042	30.072	30.04667	0.008346
40.097	40.016	40.011	40.04133	0.011123
50.093	50.0058	50.085	50.06127	0.013906
60.035	60.047	60.162	60.08133	0.016689
70.039	70.013	70.024	70.02533	0.019451
80.093	80.015	80.028	80.04533	0.022235

Theoretical Flowrate, Q_t

Y_o (cm)	V at $0.5Y_o$ (cm/s)	Q at $0.5Y_o$ (m ³ /s)
34.5	2.1	0.00217
35.6	2.1	0.00224
37.2	6.2	0.00692
38.5	7.0	0.00809
39.6	11.1	0.01319
40.5	13.6	0.01652
41.6	15.2	0.01897
42.3	16.9	0.02145
43.1	19.4	0.02508

Water Depth at Upstream and Downstream Section

y_{u1} (cm)	y_{u2} (cm)	$y_{u(average)}$ (cm)	y_{d1} (cm)	y_{d2} (cm)	$y_{d(average)}$ (cm)
34.5	34.5	34.50000	2.0	1.8	1.90000
35.6	35.5	35.55000	2.2	1.8	2.00000
37.2	37.1	37.15000	2.0	1.7	1.85000
38.5	38.5	38.50000	2.5	2.2	2.35000
39.5	39.5	39.50000	3.0	2.4	2.70000
40.4	40.5	40.45000	3.9	2.6	3.25000
41.3	41.5	41.40000	4.1	3.0	3.55000
42.1	42.2	42.15000	4.8	3.4	4.10000
42.9	42.8	42.85000	4.6	3.5	4.05000

Energy loss Between Upstream and Downstream

$y_{u(average)}$ (cm)	V upstream (m/s)	E upstream (m)	$y_{d(average)}$ (cm)	V downstream (m/s)	E downstream (m)	E loss (m)
34.50000	0.02103	0.345023	1.90000	0.38132	0.02641	0.31457
35.55000	0.06208	0.355696	2.00000	0.37380	0.02712	0.30236
37.15000	0.07000	0.37175	1.85000	1.09829	0.08248	0.26426
38.50000	0.11128	0.385631	2.35000	1.05686	0.08243	0.21779
39.50000	0.13617	0.395945	2.70000	1.62800	0.16209	0.19433
40.45000	0.15273	0.405689	3.25000	1.69477	0.17889	0.16436
41.40000	0.16960	0.415466	3.55000	1.78118	0.19720	0.11934
42.15000	0.19513	0.423441	4.10000	1.80980	0.20644	0.10321
42.85000	0.21243	0.4308	4.05000	1.94451	0.23572	0.07319

Table 5: Results of Experiment with Design Model 3

Actual Flowrate, Q_a

Q_1 (m ³ /hr)	Q_2 (m ³ /hr)	Q_3 (m ³ /hr)	Q_{ave} (m ³ /hr)	Q_{ave} (m ³ /s)
5.08020	5.07050	5.03000	5.06023	0.001406
10.00300	10.08000	10.01600	10.03300	0.002787
20.04800	20.08000	20.00600	20.04467	0.005568
30.39800	30.40800	30.40900	30.40500	0.008446
40.22600	40.16300	40.05500	40.14800	0.011152
50.31600	50.23300	50.11600	50.22167	0.01395
60.04300	60.12400	60.41100	60.19267	0.01672
70.00700	70.15400	70.41100	70.19067	0.019497
80.05900	80.10600	80.22500	80.13000	0.022258

Theoretical Flowrate, Q_t

Y_o (cm)	V at $0.5Y_o$ (cm/s)	Q at $0.5Y_o$ (m ³ /s)
34.50000	2.10000	0.00217
35.60000	4.50000	0.00481
37.20000	7.00000	0.00781
38.50000	8.60000	0.00993
39.60000	11.10000	0.01319
40.50000	13.60000	0.01652
41.60000	15.20000	0.01897
42.30000	16.90000	0.02145
43.10000	19.40000	0.02508

Water Depth at Upstream and Downstream Section

y_{u1} (cm)	y_{u2} (cm)	$y_{u(average)}$ (cm)	y_{d1} (cm)	y_{d2} (cm)	$y_{d(average)}$ (cm)
34.50000	34.50000	34.50000	2.70000	2.60000	2.65000
35.50000	35.60000	35.55000	2.80000	2.90000	2.85000
37.10000	37.20000	37.15000	2.00000	2.60000	2.30000
38.50000	38.50000	38.50000	2.50000	2.80000	2.65000
39.50000	39.50000	39.50000	3.00000	3.50000	3.25000
40.50000	40.40000	40.45000	3.90000	4.00000	3.95000
41.50000	41.30000	41.40000	4.10000	4.20000	4.15000
42.20000	42.10000	42.15000	4.80000	4.40000	4.60000
42.80000	42.90000	42.85000	4.60000	5.10000	4.85000

Energy loss Between Upstream and Downstream

$y_{u(average)}$ (cm)	V upstream (m/s)	E upstream (m)	$y_{d(average)}$ (cm)	V downstream (m/s)	E downstream (m)	E loss (m)
34.50000	0.04506	0.345104	2.65000	0.27340	0.03031	0.31457
35.55000	0.07009	0.35575	2.85000	0.56211	0.04460	0.30236
37.15000	0.08600	0.371877	2.30000	1.13217	0.08833	0.26426
38.50000	0.11128	0.385631	2.65000	1.24943	0.10607	0.21779
39.50000	0.13617	0.395945	3.25000	1.35249	0.12573	0.19433
40.45000	0.15273	0.405689	3.95000	1.39443	0.13860	0.16436
41.40000	0.16960	0.415466	4.15000	1.52366	0.15983	0.11934
42.15000	0.19513	0.423441	4.60000	1.55407	0.16909	0.10321
42.85000	0.21243	0.4308	4.85000	1.72400	62-	0.07319